ADAPTIVE MULTIPLE-INPUT MULTIPLE-OUTPUT (MIMO) TECHNIQUES FOR VISIBLE LIGHT COMMUNICATIONS

A Thesis

by

Mohamed Al-Nahhal

Submitted to the
Graduate School of Sciences and Engineering
In Partial Fulfillment of the Requirements for
the Degree of

Master of Science

in the
Department of Electrical and Electronics Engineering

Özyeğin University
August 2020

ADAPTIVE MULTIPLE-INPUT MULTIPLE-OUTPUT (MIMO) TECHNIQUES FOR VISIBLE LIGHT COMMUNICATIONS

Approved by:

Professor Murat Uysal, Advisor
Department of Electrical and Electronics Engineering
Özyeğin University

Assistant Professor Kadir Durak
Department of Electrical and Electronics Engineering
Özyeğin University

Associate Professor Ertugrul Basar
Department of Electrical and Electronics Engineering
Koç University

Date Approved: 18 August 2020

I dedicate this thesis to my beloved parents and big brother, who have instilled in me the desire to learn and helped me in everything great and small.

ABSTRACT

Visible Light Communication (VLC) technology is a promising solution of wireless communication systems in beyond 5G communication networks, which provides a low implementation cost, high energy efficiency, and high-speed data transmission. The VLC can be considered as a complementary or alternative technology for the existing Radio Frequency (RF) based wireless communication systems to satisfy the demands of increasing the high capacity. In the VLC systems, Light-Emitting Diodes (LEDs) are used as transmitters, and Photodetectors (PDs) are used as receivers. Multiple LEDs are installed to offer sufficient illumination for indoor environments. This feature can be utilized to implement Multiple-Input Multiple-Output (MIMO) communications systems in order to achieve high data rates by improving spectral efficiency. However, LEDs can only convey unipolar signals. Furthermore, the nature of the VLC channel is frequency-selective, which causes significant degradation in the performance of the VLC system due to critical Inter-Symbol Interference (ISI). Several schemes based on pulse modulation and Orthogonal Frequency Division Multiplexing (OFDM) have been proposed to overcome the ISI of the VLC system. A new Optical Orthogonal Frequency Division Multiplexing (O-OFDM), referred to as a Unipolar Orthogonal Frequency Division Multiplexing (U-OFDM), appears as an attractive solution for emerging VLC systems. In the future of 5G and beyond 5G communication networks, the spectral efficiency needs further improvement through MIMO with adaptive transmission technique.

Motivated by these, we focus on improving the spectral efficiency and Bit Error Rate (BER) performance for the MIMO VLC systems in both the single-carrier and multi-carrier. Firstly, we propose a novel Adaptive Spatial Modulation (ASM) scheme, referred to as Flexible Generalized Spatial Modulation (FGSM), for single-carrier MIMO VLC systems

to achieve better average Symbol Error Rate (SER) and higher spectral efficiency with a fixed overall number of LEDs compared to existing ASM and Generalized Spatial Modulation (GSM) schemes. The proposed system varies the modulation sizes over the available LEDs as well as the number of active LEDs. The selection of the modulation sizes is based on an optimization problem for the average SER under a predefined value of the spectral efficiency. We derive a closed-form expression of the approximate average SER for the proposed system and evaluate its decoding complexity. We show that the FGSM scheme can be a potential candidate for future MIMO-VLC systems.

Secondly, we firstly propose adaptive transmission technique for the MIMO VLC system in conjunction with U-OFDM to exploit the U-OFDM benefits. The proposed adaptive MIMO U-OFDM VLC system is implemented to support three different MIMO modes that enable a set of different modulation sizes. The considered MIMO modes are Repetition Coding (RC), Spatial Multiplexing (SMUX) and Spatial Modulation (SM). In the RC, the same signal is transmitted simultaneously from all LEDs, while independent signals are transmitted simultaneously from all LEDs in the SMUX. In the SM technique, a single LED is activated and the index of the activated LED carries information in addition to modulated signals. Depending on the received Signal-to-Noise Ratio (SNR) and target BER, the proposed adaptive transmission system switches between the available MIMO modes and adjusts its modulation size to achieve higher spectral efficiency. The proposed U-OFDM system is applied over different VLC MIMO setups with realistic channel models for 8×8, 4×4 and 2×2 MIMO systems.

Recently, Generalized LED Index Modulation (GLIM) appears as an attractive MIMO OFDM scheme for emerging VLC systems. Therefore, in the last part of this thesis, we propose a Magnitude and Wrap-Phase OFDM (MW-OFDM) scheme for the MIMO VLC systems. The proposed MW-OFDM scheme relies on the conversion of complex signals into a polar form with the magnitudes and wrap-phases to decrease the restriction on the number of LEDs compared to the conventional GLIM-OFDM. Moreover, the Maximum

Likelihood (ML) estimator for the proposed scheme is derived. The proposed MW-OFDM scheme improves the average bit error rate and provides a significant reduction in the decoding complexity, compared to the conventional GLIM-OFDM. Moreover, a half number of LEDs are required for the proposed scheme to deliver the same spectral efficiency in a comparison with the conventional GLIM-OFDM.

ÖZETÇE

Görünür Işık Haberleşme (VLC) teknolojisi; 5G'nin ötesindeki ağlarda kablosuz iletişim sistemlerinin umut verici bir çözümüdür. Düşük uygulama maliyeti, yüksek enerji verimliliği ve yüksek hızla veri iletimi sağlar. VLC sistemleri, yüksek kapasitenin artırılması taleplerini karşılamak için mevcut Radyo Frekansı (RF) tabanlı kablosuz iletişim sistemleri için tamamlayıcı veya alternatif olarak düşünülebilir. VLC sistemlerinde, ışık yayan Diyotlar (LED'ler) geri-verici olarak ve Fotodetektörler (PD'ler) alıcı olarak kullanılır. İç mekan ortamları için yeterli aydınlatma sağlamak üzere birden fazla LED monte edilmiştir. Bu özellik, spektral verimliliği artırarak yüksek veri hızlarına ulaşmak için Çok Girişli Çok Çıkışlı (MIMO) iletişim sistemlerini uygulamak için kullanılabilir. Ancak, LED'ler yalnızca tek kutuplu sinyalleri iletebilir. Ayrıca, VLC kanalının doğası frekans seçicidir, bu da kritik Semboller Arası Girişim (ISI) nedeniyle VLC sisteminin performansında önemli ölçüde bozulmaya neden olur. VLC sisteminin ISI'sinin üstesinden gelmek için darbe modülasyonu ve Ortogonal Frekans Bölmeli Çoğullamaya (OFDM) dayanan birkaç şema önerilmiştir. Yeni Optik Ortogonal Frekans Bölmeli Çoğullama (O-OFDM), Tek Kutuplu Ortogonal Frekans Bölmeli Çoğullama (U-OFDM) olarak adlandırılan, ortaya çıkan VLC sistemleri için çekici bir çözüm olarak görülmektedir. 5G'nin geleceğinde ve 5G iletişim ağlarının ötesinde, spektral verimliliğin adaptif iletim tekniği ile MIMO aracılığıyla daha da geliştirilmesi gerekmektedir.

Bunları motive ederek, öncelikle MIMO VLC sistemlerinin daha iyi ortalama Symbol Error rate (SER) ve daha yüksek spektral verimlilik elde etmek için sabit bir toplam sayıda Mevcut ASM ve Generalized Spatial Modulation (GSM) şemalarıyla karşılaştırıldığında LED'ler. Önerilen sistem, mevcut LED'lerin yanı sıra aktif LED'lerin sayısına göre modülasyon boyutlarını değiştirir. Modülasyon boyutlarının seçimi, spektral verimliliğin önceden

tanı-mlanmış bir değeri altında ortalama SER için bir optimizasyon problemine dayanmaktadır. Önerilen sistem için yaklaşık ortalama SER'nin kapalı formda bir ifadesini türetiriz ve kod çözme karmaşıklığını değerlendiririz. FGSM şemasının gelecekteki MIMO-VLC sistemleri için potansiyel bir aday olabileceğini gösteriyoruz.

İkinci olarak, U-OFDM avantajlarından yararlanmak için MIMO VLC sistemi için U-OFDM ile birlikte uyarlamalı iletim tekniği öneriyoruz. Önerilen uyarlanabilir MIMO U-OFDM VLC sistemi, bir dizi farklı modülasyon boyutu sağlayan üç farklı MIMO modunu desteklemek için uygulanır. Dikkate alınan MIMO modları Tekrar Kodlama (RC), Mekansal Çoklama (SMUX) ve Mekansal Modülasyon (SM) 'dir. RC'de, aynı sinyal tüm LED'lerden eşzamanlı olarak iletilirken, bağımsız sinyaller SMUX'daki tüm LED'lerden aynı anda iletilir. SM tekniğinde, tek bir LED etkinleştirilir ve etkinleştir-ilen LED'in dizini modüle edilmiş sinyallerin yanı sıra bilgi taşır. Alınan Sinyal-Gürültü Oranına (SNR) ve hedef Bit Hata Oranına (BER) bağlı olarak, önerilen uyarlamalı iletim sistemi mevcut MIMO modları arasında geçiş yapar ve daha yüksek spektral verimlilik elde etmek için modülasyon boyutunu ayarlar. Önerilen U-OFDM sistemi, 8×8, 4×4 ve 2×2 MIMO sistemleri için gerçekçi kanal modellerine sahip farklı VLC MIMO kurulumlarına uygulanır.

Son zamanlarda, Generalized LED Index Modulation (GLIM), ortaya çıkan VLC sistemleri için çekici bir MIMO OFDM şeması olarak ortaya çıkmaktadır. Bu nedenle, bu tezin son bölümünde, MIMO VLC sistemleri için bir Magnitude and Wrap-Phase OFDM (MW-OFDM) şeması öneriyoruz. Önerilen MW-OFDM sistemi, geleneksel GLIM-OFDM'e kıyasla LED sayısındaki kısıtlamayı azaltmak için karmaşık sinyalin büyüklüğe ve sargı fazına dönüştürülmsini kullanır. Ayrıca, önerilen şema için bir ML Tahmincisi (MLE) türetilir. Geleneksel GLIM ile karşılaştırıldığında, önerilen MW-OFDM aynı spektral verimliliği sağlamak ve aynı zamanda ortalama BER'i geliştirmek için yarım sayıda LED gerektirir. Ayrıca, önerilen MW-OFDM'in kod çözme karmaşıklığı geleneksel GLIM-OFDM ile kıyaslandığında önemli ölçüde azalır.

ACKNOWLEDGEMENTS

I would like to express my deepest gratitude and sincere appreciation to my advisor, Prof. Murat Uysal as well as Prof. Ertugrul Basar, for their wisdom, encouragement, support, patience guidance, invaluable insights, immense knowledge, and suggestions during this experience as an M.Sc. student and research assistant. The work of the thesis would not be possible without their consistent support and guidance. I also had a great opportunity to work with them. I have learned a lot from them throughout my studies. I am also grateful for technical and non-technical discussions with my colleagues in the Communication Theory and Technologies (CT&T) research group at Özyeğin university.

I am very gratefully acknowledge the funding received towards my M.Sc. from The scientific and Technological Research Council of Turkey (TÜBİTAK) under Grant 215E311.

My warmest gratitude goes to my family, who always supported me unconditionally throughout my life. Their sacrifice was great. The distances separated us, so I could not see them during the period of master studies, and they could not attend the thesis defense. I will be forever indebted to my family for their unlimited trust and willingness to endure with me the difficulties and stresses of my endeavors. Finally, I would like to thank my friends and my relatives for supporting me.

ACRONYMS

ASM	Adaptive Spatial Modulation
ACO-OFDM	Asymmetrically Clipped Optical OFDM
AWGN	Additive White Gaussian Noise
BER	Bit Error Rate
b/s/Hz	Bits per Second per Hertz
b/s	Bits per Second
bpcu	Bits per Channel Use
DC	Direct Current
DCO-OFDM	DC-biased optical OFDM
FFT	Fast Fourier Transform
FGSM	Flexible Generalized Spatial Modulation
GSM	Generalized Spatial Modulation
GLIM	Generalized LED Index Modulation
Gbit/sec	Gigabits per Second
IFFT	Inverse Fast Fourier Transform
IM/DD	Intensity Modulation/Direct Detection
ISI	Inter-Symbol Interference
LED	Light-Emitting Diode
ML	Maximum Likelihood
MAP	Maximum A Posterior Probability
MW-OFDM	Magnitude and Wrap-Phase OFDM
MCM	Multicarrier Modulation
MMSE	Minimum Mean Square Error

Mb/s	Megabits per Second
MIMO	Multiple-Input Multiple-Output
OFDM	Orthogonal Frequency Division Multiplexing
O-OFDM	Optical Orthogonal Frequency Division Multiplexing
OWC	Optical Wireless Communication
OOK	On-Off Keying
PSD	Power Spectral Density
OSIC	Optimal Ordering Successive Interference Cancellation
PDF	Probability Density Function
PAM	Pulse Amplitude Modulation
PD	Photodetector
P-OFDM	Polar OFDM
PSK	Phase Shift Keying
P/S	Parallel-To-Serial
QAM	Quadrature Amplitude Modulation
RC	Repetition Coding
RF	Radio Frequency
S/P	Serial-To-Parallel
SMUX	Spatial Multiplexing
SM	Spatial Modulation
SER	Symbol Error Rate
SISO	Single-Input Single-Output
SNR	Signal-to-Noise Ratio
U-OFDM	Unipolar Orthogonal Frequency Division Multiplexing
VLC	Visible Light Communication
ZF	Zero-Forcing

TABLE OF CONTENTS

LIST OF TABLES

LIST OF FIGURES

LIST OF ALGORITHMS

CHAPTER I

INTRODUCTION

1.1 Motivation

In the last decade, wireless services and the number of mobile devices have increased exponentially around the world, which demanded a significant increase in data transfer based wireless technologies [1]. Earlier, in most cases, RF technology has satisfied this demand. However, RF technology has limited bandwidth and in some scenarios causes interference, such as in airports and hospitals. Meanwhile, the industry of illumination has been developed due to the LEDs which are more popular, highly reliable, economical, energy-efficient, accessible, and have a significantly longer lifetime than classical light sources [2]. In this context, VLC is a new wireless technology that uses LEDs for both illuminations and wireless data transmission purposes. LED-based VLC technology considers as a complementary or alternative promising solution for the current RF systems, which offers a free spectrum, high energy efficiency, high data rate transmission, low implementation cost, and huge bandwidth [3].

Several researchers have efforted towards VLC systems development due to its advantages over RF systems. However, there are several challenges that hinder the VLC development and should be addressed. Among these challenges, the characteristics of LEDs which can only transfer unipolar signals, and therefore, the VLC system have relied on intensity modulation and direct detection. On-Off Keying (OOK) and other pulse modulation formats have been considered to deal with the constraints of LEDs [4]. Another challenge to VLC systems, the VLC channel is frequency-selective naturally that causes significant degradation for the performance of the VLC system due to critical the ISI. OFDM-based VLC has been proposed to mitigate the ISI for VLC systems [5, 6].

Typically, multiple LEDs are installed to offer sufficient illumination for indoor environments. This feature can be utilized to implement the MIMO communications systems in order to achieve high-data rates by improving the spectral efficiency [7–9]. In the future of 5G and beyond 5G communication networks, the spectral efficiency needs further improvement through MIMO with adaptive transmission technique [10]. Consequently, the objective of this thesis is to exploit the advantages of VLC and overcome its faced challenges. This can be done by proposing and evaluating novel and efficient techniques to enhance the VLC performance systems over realistic VLC channels in terms of BER/SER and spectral efficiency.

1.2 Overview on Optical Wireless communications

Wireless communication technologies, such as wireless devices, applications and services, have already become an important part of our daily life. Therefore, broadband internet services require further novel promising wireless technologies capable of satisfying the users' increased demands. The existing RF-based wireless communication technologies suffer from some limitations. One of the limitations is the bandwidth of these technologies with available spectrum congestion. Thus, these technologies inadequate even for the demands of the existing applications and not to mention future demands. This limitation is more equate in the indoor wireless applications which there is an insufficiency enough of bandwidth to cover the demands of users. Consequently, highly reliable wireless technologies and low implementation costs are needed for indoor wireless communications [6].

Optical Wireless Communication (OWC) technology is an alternative or complementary solution to overcome the restrictions of RF technologies. OWC technologies offer unlimited bandwidth suitable for satisfying the increased demands, robustness to electromagnetic interference and inherent physical security, compared to the RF counterparts [11, 12]. In addition, OWC technologies have free licensing due to operating in the unregulated spectrum which leads to the reduction of implementation cost for several applications. For

instance, in the indoor room environment, the wireless link utilizes the high SNR given by the LEDs of the room illumination instead of utilizing high power RF base stations. The OWC systems include a VLC technology that operating in the visible band that ranged from 390 nm to 750 nm as shown in Figure 1. VLC systems can offer very high-speed data transmission without any noteworthy effects on the room illumination and human eye.

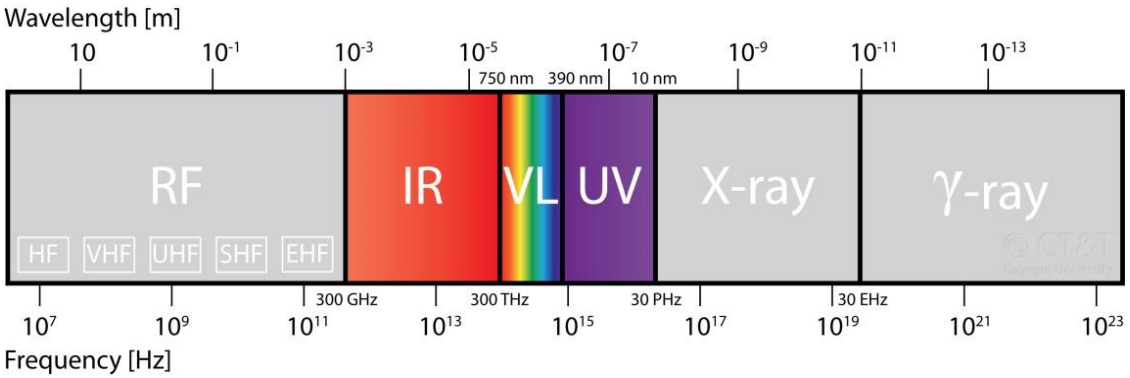

Figure 1: The electromagnetic spectrum distribution.

1.3 Visible Light Communications

VLC is a new OWC technology that uses the efficient-energy LEDs for illumination services and wireless communication transmission purposes. VLC offers several advantages, such as: huge bandwidth due to the visible light frequency spectrum ranges 430 THz and 790 THz; high power and wireless data transmission; free license which not limited by any law; safe for the human body; low implementation cost.

1.3.1 Fundamentals of VLC

In the VLC systems, the VLC transmitter modulates the light beam resulted from LEDs and the VLC receiver that uses the PDs in order to retrieve the modulated signal from the light beam. Consequently, the VLC systems rely on Intensity Modulation/Direct Detection

(IM/DD) for transmission. The connection between the VLC transmitter and the VLC receiver is through the VLC channel.

The prime functionality for the VLC transmitter is converting the electrical signal into an optical signal, and then, conveys the resulted optical signal through the LEDs into the VLC channel. The LEDs in the VLC system have several advantages, such as low cost and safe for the human eye even at high powers [13]. In addition, the LEDs are more reliable compared to the conventional light bulbs. However, the LEDs suffer from some limitations, such as only unipolar signals that can be transmitted through LEDs, low modulation bandwidth (few tens of MHz), low-efficiency for electrical-to-optical power conversion (ranged from 10% to 40%) and non-linearity [14]. In the VLC receiver, the received optical signal is converted into an electrical signal by the PDs, and then, the resulted electrical signal is passed by estimator and demodulator in order to extract the original data information.

1.3.2 Indoor VLC Channel Model

The characteristics of the VLC channel modeling is basically essential to evaluate the VLC system performance from a signal integrity point of view. Several VLC channels modeling have been studied in the literature. In [15–18], the recursive method has been adopted in order to get the channel impulse response in the visible band. In [19], a novel frequency-domain method has been proposed, where the channel transfer functions of both diffuse and direct line-of-sight components are considered. Geometric models have been proposed in [20–22] for the VLC channels in order to calculate the non-line-of-sight channel impulse response. A Monte-Carlo ray tracing simulation tool has been proposed in [23,24] in order to get the channel impulse response for the VLC, which considers Lambertian sources and wavelength dependency of reflectance.

Recently, realistic VLC channels models have been studied based on Zemax® software [25–27]. This software contains two models of ray tracing which are sequential ray

tracing and non-sequential ray tracing. In the sequential ray tracing, rays are traced during a sequence of surfaces, where each surface is hit only once during the traveling from the transmitter to the receiver. In the non-sequential ray tracing, rays are allowed to be propagated, scattered, and reflected through the room environment with any order.

In order to model the indoor environment (e.g., office room, living room, etc.) using Zemax®, we should specify the dimensions and shape of the room and other objects (i.e., walls, ceiling, furniture, etc.). In addition, the kind of surface materials within the room should be specified. As well as the properties and locations of the LEDs and PDs should specify. After creating the indoor environment by using Zemax®, we utilize the non-sequential ray tracing of Zemax® to obtain the channel impulse response.

An example of the indoor VLC channel which has been developed in [28]. An office space with dimensions of 5 m×5 m×3 m (see Figure 2(a) on the next page) is considered with 16 LED ceiling light sources (see Figure 2(b) on the following page). It is assumed 17 Watts for each LED which realizes illumination standard in the range of $365-612$ lux obeying the illuminating engineering society of North America standard. A laptop computer is considered as a destination terminal which is placed on the desk and is linked to 4 USB hubs each of is provided with 4 PDs (see Figure 3 on page 7). The separation between adjacent PDs is set either as 3 cm or 5 cm each with 0.07 cm^2 surface area, whereas the distance between neighboring USB hubs sets to 12.5 cm [28]. The other specifications are abstracted in Table 1 on page 7. For the simulation studies of this thesis, different MIMO setups are considered by choosing some subsets of the general 16×16 MIMO system.

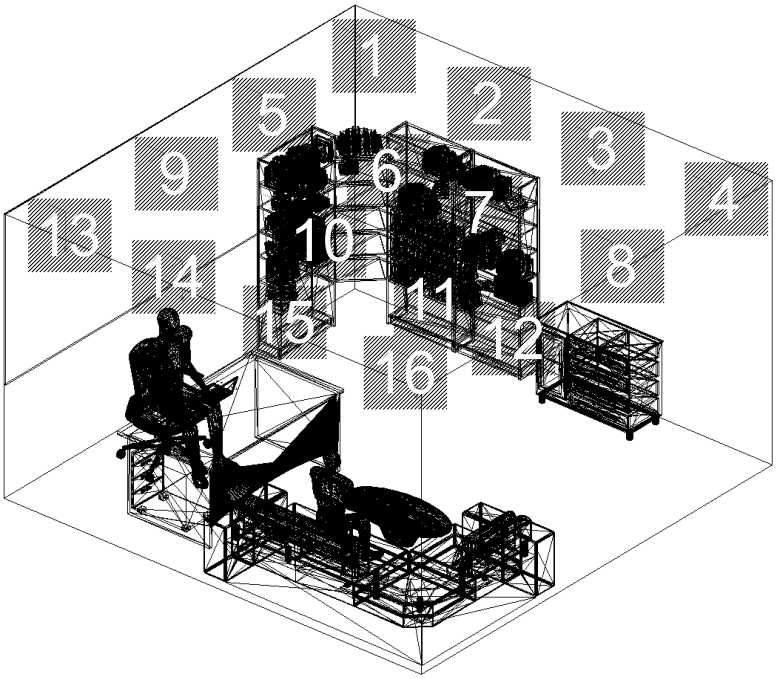

(a)

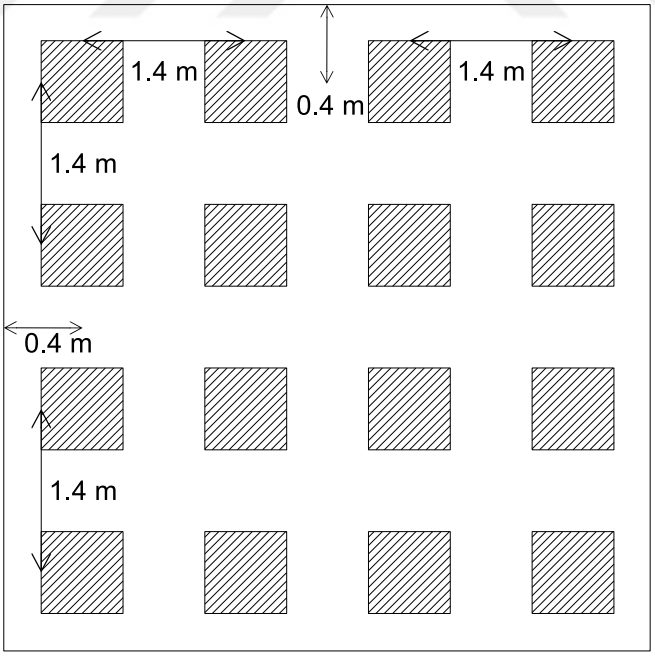

(b)

Figure 2: (a) Top view of office room and (b) arrangement of luminaries [28].

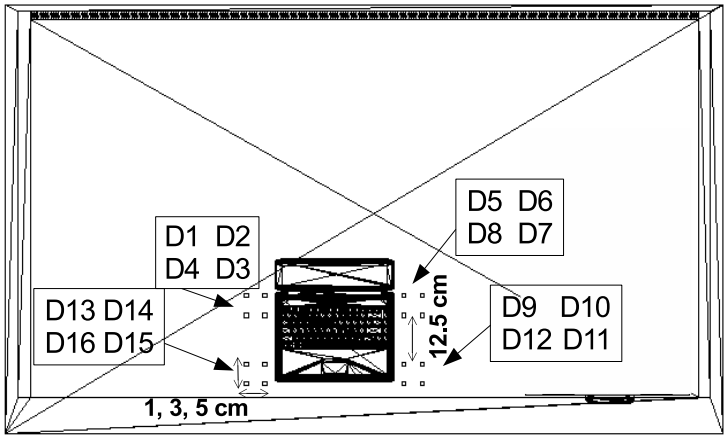

Figure 3: Top view of the desk with laptop computer and PDs labeled from 1 to 16 [28].

Table 1: Specifications of office room model.

Room size	5 m×5 m×3 m.
Materials	Walls: Plaster, Ceiling: Plaster. Floor: Pinewood, Desk: Pinewood.
Objects	1 desk and a chair paired with desk. 1 laptop on the desk, 1 desk light on the desk. 1 library, 1 couch, 1 coffee table. 1 widow, 2 human bodies.
Specifications of objects	Desk: Pinewood (Height 0.88 m). Chair: Black gloss paint, Laptop: Black gloss paint. Desk light: Black gloss paint. Library: Pinewood, Window: Glass. Couch: Cotton, Coffee table: Pinewood. Human body: Head, Hands (assumed to be absorbing). Clothes (cotton), Shoes (black gloss).
Specifications of luminary	17 Watt, Brand: LR24-38SKA35 Cree Inc. Half viewing angle: 40°.

1.4 VLC Modulation Schemes

The VLC systems channels are quite different from conventional RF systems channels, where VLC systems are based on the IM/DD for the data wireless transmission [29, 30]. Thus, the signals of the O-OFDM should be transmitted as unipolar (i.e, positive real-valued) signals. Consequently, different techniques of modulation schemes are used. Some of the modulation schemes suitable for RF systems channels are not proceeding well in the VLC systems. The most important factor to choose suitable modulation scheme for the VLC system is the capability of dealing with the limitation of LEDs at the transmitter side as mentioned in Section 1.3.1. This part discusses the most popular modulation schemes used for the VLC systems. We discuss the baseband modulation scheme, such as unipolar Pulse Amplitude Modulation (PAM), and the optical Multicarrier Modulation (MCM) scheme, such as DC-biased optical OFDM (DCO-OFDM), Asymmetrically Clipped Optical OFDM (ACO-OFDM) and U-OFDM.

1.4.1 Unipolar Pulse Amplitude Modulation

The unipolar PAM modulation scheme is one of the most widely used modulation schemes for VLC systems due to its simplicity [31, 32]. The OOK is the special case of unipolar PAM, which only has two levels (i.e., ”zero” or ”one”) and has been used in the IEEE 802.15.7 standard [33].

In the unipolar M-PAM VLC system (where $M = 2^b$ is the modulation size, b is a positive integer value that represents the number of bits per symbol), the transmitted signal, $x(t)$, can be expressed as $x(t) = s_m p(t)$, where $m \in \{0, \ldots, M-1\}$ and $p(t)$ represents the pulse shaping. Here, s_m denotes the constellation symbol of PAM scheme and $s_m = m$ is considered. The average electrical energy per symbol, E_s, can be calculated as $E_s = (\varepsilon_p/6)(M-1)(2M-1)$, where ε_p represents the energy of pulse shaping $p(t)$ [3, 4].

In the presence of Additive White Gaussian Noise (AWGN) channel only, the BER of

unipolar PAM for VLC systems can be represented as $\mathrm{BER}_{PAM} \approx \frac{2(M-1)}{M\log_2(M)} Q\left(d_{\min}/\sqrt{2N_0}\right)$, where N_0 is the Power Spectral Density (PSD) of AWGN; $Q(x)$ denotes the tail Probability Density Function (PDF) of the standard Gaussian distribution with a zero mean and unity variance, and can be expressed as $Q(x) = (1/\sqrt{2\pi}) \int_y^{\infty} \exp\left(-y^2/2\right) dy$; $d_{\min}$ is the minimum Euclidean distance between different constellation symbols of PAM. Assume the Gray mapping is employed, the $d_{\min}$ can be calculated as $d_{\min} = \sqrt{6E_s/((M-1)(2M-1))}$ [4, 34]. Let $\gamma = E_s/N_0$ defines the average SNR. Therefore, the BER of unipolar PAM becomes $\mathrm{BER}_{PAM} \approx \frac{2(M-1)}{M\log_2(M)} Q\left(\sqrt{3\gamma/((M-1)(2M-1))}\right)$.

In the OOK modulation scheme (an especial case of PAM), the zeros and ones probabilities are equiprobable. Thus, the optimal threshold level in the midway is considered and the BER of OOK can be represented as $\mathrm{BER}_{OOK} = Q\left(\sqrt{\gamma}\right)$ [12].

1.4.2 Optical OFDM

The optical MCM schemes consider more efficient than the basband modulation schemes. The complex modulation schemes, such as Phase Shift Keying (PSK) and Quadrature Amplitude Modulation (QAM) modulation schemes, can be used with the O-OFDM schemes. The nature of the VLC channel is frequency selective which causes the ISI. The O-OFDM schemes offer strong immunity against the ISI which results in improving the VLC system performance. The conventional OFDM scheme is reformulated to be suitable for VLC systems due to the IM/DD restriction which requires only unipolar signals for transmission through LEDs [3, 35–37]. Several O-OFDM formats have been introduced for the VLC systems. However, the existing O-OFDM formats either sacrifice power as adding a required Direct Current (DC) bias or sacrifice spectral efficiency in order to satisfy unipolar constrains. Therefore, in the O-OFDM VLC systems, the spectral efficiency and power are a tradeoff. The most popular formats of the O-OFDM schemes used in the VLC systems are DCO-OFDM, ACO-OFDM [5, 38–40] and U-OFDM [41].

In the DCO-OFDM, ACO-OFDM and U-OFDM systems, binary information is first

mapped to complex symbols using any complex modulation, such as PSK or QAM. The complex-valued modulated symbols are applied to Hermitian symmetry before Inverse Fast Fourier Transform (IFFT), for extracting a real-valued bipolar signal. A cyclic prefix with the size is appended to the real-valued bipolar signal in order to overcome the ISI.

In order to solve the bipolarity problem, the DCO-OFDM system uses the DC bias subsequent to the IFFT. Whereas the ACO-OFDM significantly reduces the required DC bias at the expense of sacrificing half of the spectral efficiency, compared to DCO-OFDM.

In the U-OFDM system, the resulting real-valued bipolar signal is converted into a unipolar signal by doubling the original OFDM frame. The first OFDM frame refers to the positive samples and the second one represents negative samples. In the first frame, the negative samples set as inactive (i.e., set to zero). In the second OFDM frame, the positive samples set as inactive and the negative samples are multiplied by -1 to be positive (see Figure 4). Then, the resulting signal propagates through the optical VLC channel to the PDs. At the receiver side, the negative frame of the U-OFDM signal is subtracted from the positive frame. After that, the reverse process will proceed in order to recover the original information.

It should be noted that the U-OFDM system is more power-efficient than DCO-OFDM. Since the U-OFDM does not require a DC bias like DCO-OFDM. This indicates that the U-OFDM can achieve a lower BER than the DCO-OFDM [6, Ch. 12] and [41].

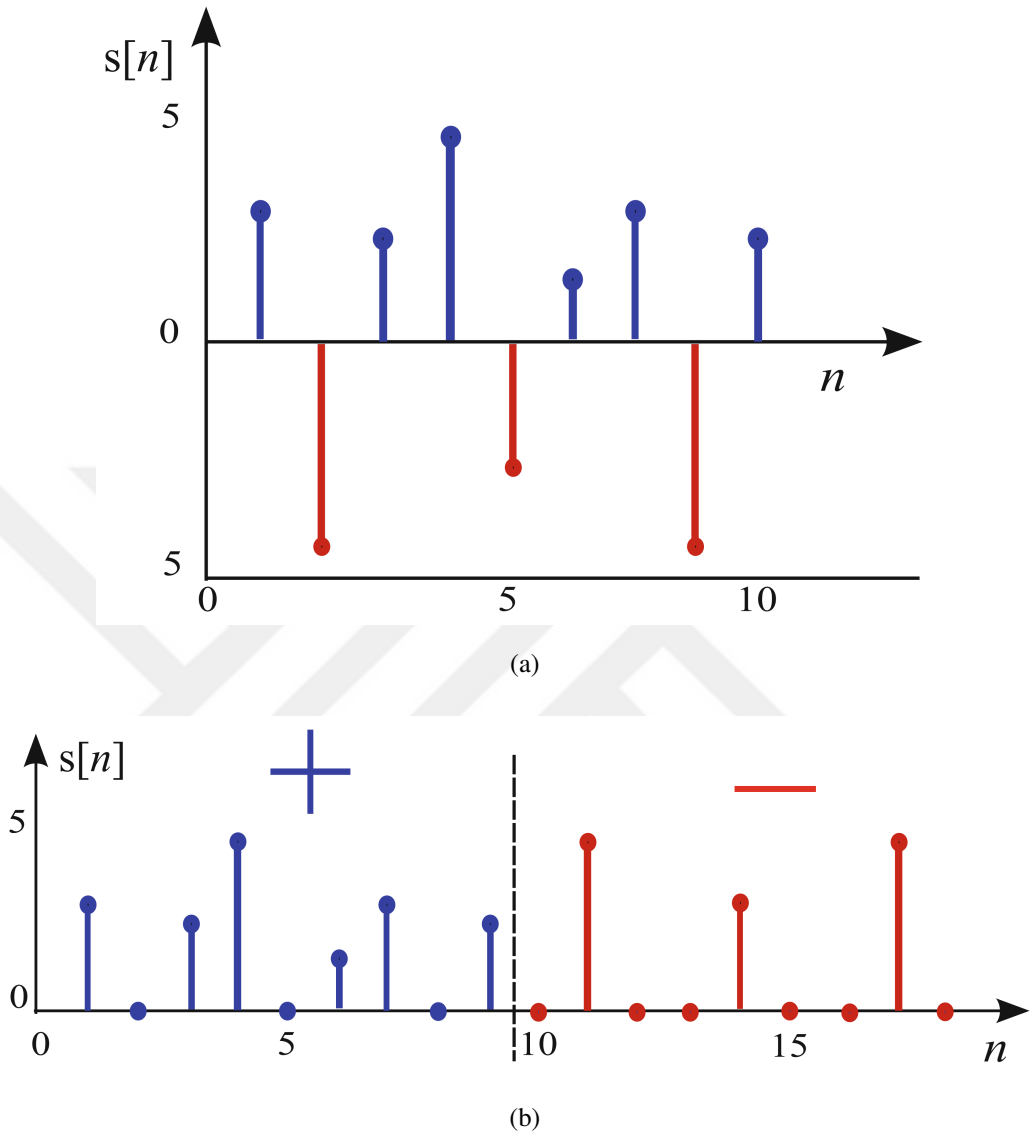

Figure 4: (a) Original bipolar OFDM signal and (b) Constructed U-OFDM signal.

1.5 Literature Review on MIMO VLC

Earlier, an initial work for the VLC field has been proposed relying upon a simple modulation scheme in order to deal with LEDs constraints namely OOK [29]. However, the VLC channel nature is a frequency-selective which causes significant degradation in the VLC system performance due to critical ISI. Several works have been proposed based on pulse modulations [42] and especially OFDM to mitigate the ISI and improve the VLC system

performance [5, 38–41, 43, 44]. An ACO-OFDM and DCO-OFDM have been proposed in [5, 38–40]. Furthermore, a flip OFDM [43], U-OFDM and enhanced U-OFDM [41, 44] have been presented for the VLC field.

In indoor environments, such as conference halls, libraries, airports and other similar public places, a large number of ceiling LEDs are typically installed to offer sufficient illumination. This makes MIMO systems a natural candidate for VLC. Performance comparison for different techniques of MIMO modes such as RC, SMUX and SM have been investigated in [7] based on a single carrier over VLC links. In RC, the same signal is transmitted simultaneously from all LEDs, while independent signals are transmitted simultaneously from all LEDs in the SMUX. In the SM technique, a single LED is activated and the index of the activated LED carries information in addition to modulated signals [6, Ch. 6]. the SM achieves a better error rate performance in comparison to SMUX while it yields a higher spectral efficiency with respect to RC. In [8], novel constellation design for MIMO VLC system has been proposed in comparison to conventional MIMO modes (RC, SMUX, and SM). A joint optimization for precoder and equalizer design of the SMUX MIMO VLC system has been studied in [9]. A GSM has been proposed in [45], where a combination of LEDs is simultaneously activated for transmission. Another variant of SM, called ASM, has been proposed in [46], where the modulation size is changed for each LED to improve the spectral efficiency.

In [47–49], the MIMO techniques have been integrated with the OFDM system for further improvement in the indoor VLC systems performances. The authors in [47] have discussed the performance of the ACO-OFDM system based on the SMUX MIMO technique using both Zero-Forcing (ZF) and Minimum Mean Square Error (MMSE) equalizers with the channel correlation effect. A precoding design for multiuser MIMO OFDM VLC system with both ZF and MMSE equalizers has been presented in [48]. In [49], performance comparison for RC, SMUX and SM modes of MIMO technique with DCO-OFDM VLC system has been presented.

In the future of 5G and beyond 5G communication networks, the spectral efficiency needs further improvement through MIMO, adaptive transmission or other techniques [10]. Adaptive transmission is a technique which utilizes one or more transmission parameters such as transmit power, modulation size, etc. for improving spectral efficiency based on channel condition quality. In the literature, the adaptive transmission has been extensively presented in RF wireless communications field. Recently, the adaptive transmission has been applied to the VLC field and particularly in conjunction with OFDM [50–54]. The authors of [50] and [51] have proposed the adaptive data rate with consideration of bit and power loading for the OFDM VLC system. In [52], the spectral efficiency improvement through adaptive modulation scheme has been studied for DCO-OFDM, ACO-OFDM, and single carrier frequency domain equalizer. An efficient coding modulation and adaptive data rate have been presented for the OFDM VLC system in [53]. The author in [54], have experimentally demonstrated an adaptive scheme enhancement with pairwise coding for the OFDM VLC system. The IEEE 802.15.13 and IEEE 802.11.bb standards for the VLC link aspiring to realize the data rate up to 10 Gigabits per Second (Gbit/sec) [10]. For achieving the required data rate, adaptive transmission based on MIMO OFDM should be adopted. In [55] and [56], the adaptive MIMO system based on respectively SMUX and SM have been investigated for single carrier over VLC link. A simple adaptive MIMO VLC system to improve energy efficiency has been presented in [57]. In [58] and [28], the adaptive transmission for MIMO DCO-OFDM VLC system has been proposed. The proposed adaptive system in [58] has been considered the SMUX of MIMO mode to improve the system performance based on the bit and power loading. Whereas in [28], the proposed adaptive system has been supported both RC and SMUX of MIMO modes for spectral efficiency enhancement.

In [59–61], the Polar OFDM (P-OFDM) technique has been proposed for Single-Input Single-Output (SISO) VLC systems, where each complex symbol resulted from IFFT is

converting into magnitude and wrap-phase. The P-OFDM achieves twice of spectral efficiency compared to the ACO-OFDM, and improves the energy-efficient of the VLC systems. In [62, 63], the idea of possibly using the magnitude and phase are triggered through multiple LEDs transmission for a single carrier. A GLIM appears as a promising scheme for MIMO OFDM VLC systems [64–66]. In the GLIM-OFDM scheme, the real and imaginary parts of the complex symbol are transmitted from separate two groups of LEDs and only one LED is active from each group. At the receiver side, the GLIM-OFDM utilizes a conditional Maximum A Posterior Probability (MAP) decoder to detect those real and imaginary parts. The GLIM-OFDM scheme achieves a higher spectral efficiency and better BER performance than the existing MIMO OFDM schemes since it does not require a Hermitian symmetry or DC bias. However, the GLIM-OFDM scheme suffers from a restriction on the number of LEDs, where it requires four LEDs to transmit one symbol. Moreover, the signs of the real and imaginary values are estimated by considering all possible active LED pair scenarios which lead to increasing the complexity of the VLC systems.

1.6 Thesis Contributions and Structure

The thesis contributions have three main parts that can be organized as follows:

In the first part of the thesis, we propose a novel ASM scheme, referred to as FGSM, for single-carrier MIMO VLC systems to achieve a better average SER and higher spectral efficiency with a fixed overall number of LEDs compared to ASM. The proposed system varies the modulation sizes over the available LEDs as well as the number of active LEDs. The selection of the modulation sizes is based on an optimization problem for the average SER under a predefined value of the spectral efficiency. We derive a closed-form expression of approximate average SER for the proposed system and evaluate its decoding complexity. We show that the FGSM scheme can be a potential candidate for future MIMO-VLC systems.

In the second part of the thesis, we propose an adaptive transmission technique for the

MIMO VLC system in conjunction with U-OFDM to exploit the U-OFDM benefits. The proposed adaptive MIMO U-OFDM VLC system is implemented to support three different MIMO modes that enable a set of different modulation sizes. The considered MIMO modes are RC, SMUX and SM. In the RC, the same signal is transmitted simultaneously from all LEDs, while independent signals are transmitted simultaneously from all LEDs in the SMUX. In the SM technique, a single LED is activated and the index of the activated LED carries information in addition to the modulated signals. Depending on the received SNR and target BER, the proposed adaptive transmission system switches between the available MIMO modes and adjusts its modulation size to achieve higher spectral efficiency. The proposed U-OFDM system is applied over different VLC MIMO setups with realistic channel models for 8×8, 4×4 and 2×2 MIMO systems.

In the third part of the thesis, we propose an MW-OFDM scheme for the MIMO VLC systems. The proposed MW-OFDM system exploits the conversion of the complex signal into a polar form with the magnitudes and wrap-phases to decrease the restriction on the number of LEDs compared to the conventional GLIM-OFDM. Moreover, the ML estimator for the proposed scheme is derived. Compared to the conventional GLIM-OFDM, the proposed MW-OFDM requires a half number of LEDs to deliver the same spectral efficiency as well as improves the average BER. Furthermore, the decoding complexity of the proposed MW-OFDM is significantly reduced in a comparison with the conventional GLIM-OFDM. We evaluate our proposed MW-OFDM scheme over realistic MIMO VLC channels.

The structure of this thesis can be organized as follows: Chapter 2 shows the FGSM scheme can be a potential candidate for future MIMO-VLC systems. Chapter 3 focuses on evaluating the performance of the proposed adaptive transmission technique for the MIMO U-OFDM VLC system which supports three different MIMO modes. Chapter 4 presents the proposed MW-OFDM scheme for the emerging MIMO VLC systems. These chapters are organized as follows:

Chapter 2 is organized as follows: In Section 2.2, we describes the system model for the proposed FGSM. In Section 2.3 and Section 2.4, we derive the closed-form expression of the approximate average SER and perform the decoding complexity analysis for the proposed FGSM, respectively. In Section 2.5, we present the numerical results to confirm the accuracy of SER derivations and to evaluate the proposed FGSM VLC system.

Chapter 3 is organized as follows: In Section 3.2, we propose the proposed adaptive MIMO U-OFDM VLC system. Section 3.3, we present the adaptive transmission algorithm. In Section 3.4, we describe the indoor MIMO VLC channel model. Section 3.5 shows the numerical results of the proposed system.

Chapter 4 is organized as follows: Section 4.2 presents the system model for the proposed MW-OFDM scheme. In Section 4.3, we derive the ML estimator for the proposed MW-OFDM. In Section 4.4, the decoding complexity analysis for the proposed MW-OFDM is performed, compared to the GLIM-OFDM schemes. Section 4.5 presents numerical results to evaluate and demonstrate the superiority of our proposed MW-OFDM scheme, compared to the existing ones.

CHAPTER II

FLEXIBLE GENERALIZED SPATIAL MODULATION FOR VISIBLE LIGHT COMMUNICATIONS

2.1 Introduction

The ASM varies the modulation size across the transmit LEDs to improve the overall spectral efficiency of VLC systems. In this chapter, we propose the so-called FGSM for VLC systems to achieve better average SER and higher spectral efficiency with a fixed overall number of LEDs compared to ASM. The proposed system varies the modulation sizes over the available LEDs as well as the number of active LEDs. The selection of the modulation sizes is based on an optimization problem for the average SER under a predefined value of the spectral efficiency. A closed-form expression of approximate SER is derived along with decoding complexity calculations for the proposed system. We show that the FGSM scheme can be a potential candidate for future MIMO-VLC systems. Numerical results are provided to confirm the superiority of the proposed system and to support theoretical derivations.

The rest of this chapter is organized as follows: In Section 2.2, we present the system model for the proposed FGSM. In Section 2.3, we derive the closed-form expression of the approximate average SER and perform the decoding complexity analysis for the proposed FGSM. In Section 2.4, the decoding complexity of the proposed FGSM is analyzed and compared with the ASM. Section 2.5 presents numerical results to confirm the accuracy of our derivations and to demonstrate the superiority of FGSM.

2.2 System Model

Consider an FGSM VLC system with L LEDs at the transmitter and P PDs at the receiver. The proposed FGSM system basically activates more than a single LED (i.e., activates a combination of LEDs) and transmits symbols from variable modulation sizes across LED combinations. The number of active LEDs at any given time is denoted by L_a, where $1 < L_a < L$. The proposed system has total of 2^{η_s} LED combinations, where $\eta_s = \left\lfloor \log_2 \binom{L}{L_a} \right\rfloor$ is the number of bits transmitted in the spatial domain (i.e., spatial spectral efficiency) and $\lfloor \cdot \rfloor$ denotes the floor operation.

The proposed system employs the unipolar PAM and LED combinations are grouped into U, $1 \leq U \leq L$, combination groups, each of which uses a different modulation size of unipolar PAM. It should be noted that available modulation sizes of unipolar PAM is $\mathbf{m} = [M(1) \dots M(U)]$, and the set of constellation symbols that can be transmitted from the u-th combination group denoted by $X(u)$ and is given as

$$X(u) \in \left\{ x_1^u, \dots, x_{M(u)}^u \right\} \quad \text{for} \quad u = 1, \dots, U, \tag{2.1}$$

where x_m^u (with the average electrical symbol energy E_s) is the m-th symbol that transmitted from the u-th combination group for $m \in \{1, \dots, M(u)\}$, and $M(u)$ represents the selected modulation size of the u-th combination group. It should be noted that the constellation symbol $x_m^u = m$ is considered.

Let g represents the LED combination and $\mathscr{I}_g$ stands for the set of indices for the active LED combination. Thus, the received signal, $\mathbf{y} \in \mathbb{R}^{P \times 1}$, can be expressed as

$$\mathbf{y} = \sum_{\mathscr{I}_g} \mathbf{h}_{\mathscr{I}_g} x_m^u + \mathbf{w}, \tag{2.2}$$

where $\mathbf{w} \in \mathbb{R}^{P \times 1}$ is the vector of AWGN samples with zero-mean and variance σ_w^2. Here, $\sum_{\mathscr{I}_g} \mathbf{h}_{\mathscr{I}_g}$ is the summation of L_a columns of the VLC channel matrix, $\mathbf{H} \in \mathbb{R}^{P \times L}$, based on the indices of $\mathscr{I}_g$.

At the receiver side, the task of the receiver is to find g (which accordingly indicates the indices of $\mathscr{I}_g$ and the combination group of u) and the transmitted symbol x_m^u. Thus, the ML decoder can be formulated as

$$\{\hat{g}, \hat{m}\} = \arg \min_{\substack{g=1,\ldots,2^{\eta_s} \\ m=1,\ldots,M(u)}} \left\| \mathbf{y} - \sum_{\mathscr{I}_g} \mathbf{h}_{\mathscr{I}_g} x_m^u \right\|^2 . \tag{2.3}$$

The number of LED combinations in each combination group u is denoted by N_u, where $\sum_{u=1}^{U} N_u = 2^{\eta_s}$. Therefore, the overall spectral efficiency, η in bpcu, of the proposed FGSM system can be calculated as

$$\eta = \left\lfloor \log_2 \binom{L}{L_a} \right\rfloor + \frac{1}{2^{\eta_s}} \sum_{u=1}^{U} N_u \log_2 M(u) . \tag{2.4}$$

Assume that the proposed FGSM system operates with $L = 8$, $L_a = 2$ ($\eta_s = 4$ bpcu), $N_1 = N_2 = 8$ (i.e., $U = 2$) and the available modulation sizes of unipolar PAM $\mathbf{m} = [4\ 32]$. Here, N_1 and N_2 represent the number of LED combinations in the first and second combination groups, respectively. Consequently, Figure 5 on the next page presents the concept of varying the available modulation sizes over the combination groups based on the values of N_1 and N_2. It should be noted that the FGSM system requires only 2^{η_s} LED combinations out of $\binom{L}{L_a}$ possibilities. For instance, in Figure 5 on the following page, the proposed system with $L = 8$ and $L_a = 2$ requires only 16 LED combinations out of 28 possibilities.

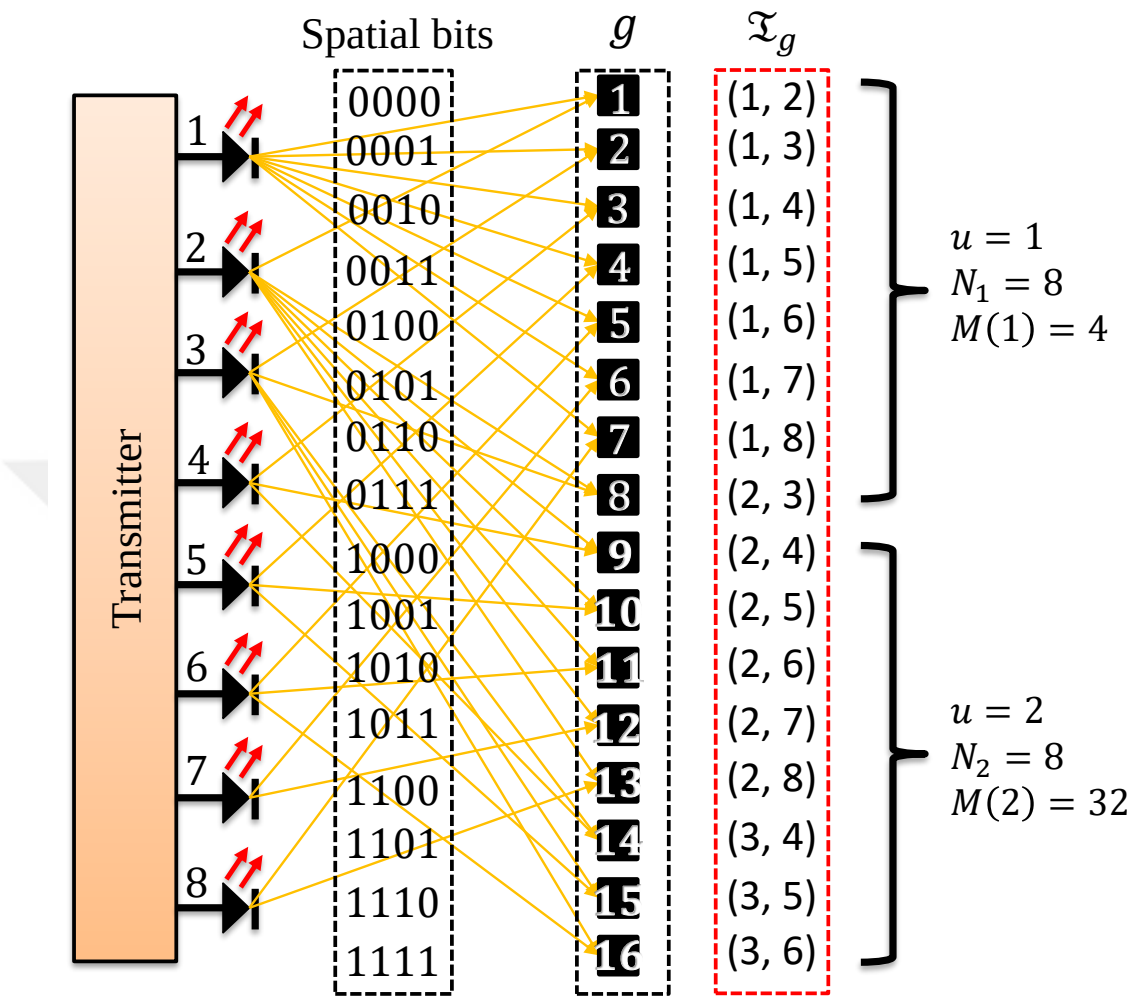

Figure 5: Proposed FGSM system for $L = 8$, $L_a = 2$, $U = 2$ and $\mathbf{m} = [4\ 32]$.

2.3 Performance Analysis

In this section, the closed-form expression of the approximate average SER is derived for the proposed FGSM system.

2.3.1 SER Performance

In the FGSM system, the approximate SER for the g-th LED combination, SER^g, can be expressed as

$$\mathrm{SER}^g \approx P(x_m^g) + P(\mathscr{I}_g) - P(x_m^g)P(\mathscr{I}_g), \quad g = 1, \ldots, 2^{\eta_s}, \tag{2.5}$$

where $P(x_m^g)$ represents the error probability of the symbol x_m^g and $P(\mathscr{I}_g)$ represents the error probability in $\mathscr{I}_g$. Here, x_m^g is the m-th symbol that transmitted from the g-th LED combination and the symbol x_m^g is considered as $x_m^g = m$, $m \in \{1, \ldots, M(g)\}$.

The error probability of the symbol x_m^g can be given as [67, Eq. (4.3-3)]

$$P(x_m^g) = Q\left(\frac{d_{\min}^g}{\sqrt{4\sigma_w^2}}\right), \tag{2.6}$$

where $d_{\min}^g$ is the minimum Euclidean distance between any two adjacent symbols. Based on the unipolar PAM constellation where $x_m^g = m$, $m \in \{1, \ldots, M(g)\}$ (i.e., $|x_1^g - x_2^g| = 1$) and under the assumption of correct index detection, $d_{\min}^g$ can be expressed as

$$d_{\min}^g = \frac{1}{\sqrt{L_a}} \left\| \sum_{\mathscr{I}_g} \mathbf{h}_{\mathscr{I}_g} \right\|. \tag{2.7}$$

By substituting Eq. (2.7) into Eq. (2.6), the error probability of the symbol x_m^g in Eq. (2.6) becomes

$$P(x_m^g) = Q\left(\frac{\left\| \sum_{\mathscr{I}_g} \mathbf{h}_{\mathscr{I}_g} \right\|}{\sqrt{4L_a\sigma_w^2}}\right). \tag{2.8}$$

The error probability in $\mathscr{I}_g$ for the m-th symbol can be represented as $Q(D_m^g/\sqrt{4\sigma_w^2})$, where D_m^g is the minimum Euclidean distance between x_m^g and all possible symbols can be transmitted from the other LED combinations. Thus, for a given combination g, D_m^g can be expressed as

$$D_m^g = \min_{\substack{i = 1, \ldots, 2^{\eta_s} \\ q = 1, \ldots, M(i) \\ i \neq g}} \frac{1}{\sqrt{L_a}} \left\| \sum_{\mathscr{I}_g} \mathbf{h}_{\mathscr{I}_g} x_m^g - \sum_{\mathscr{I}_i} \mathbf{h}_{\mathscr{I}_i} x_q^i \right\|. \tag{2.9}$$

The total error probability in $\mathscr{I}_g$ becomes

$$P(\mathscr{I}_g) = \frac{1}{M(g)} \sum_{m=1}^{M(g)} Q\left(\frac{D_m^g}{\sqrt{4\sigma_w^2}}\right). \tag{2.10}$$

Using Eq. (2.8) and Eq. (2.10) into Eq. (2.5), the closed-form expression of the approximate average SER for FGSM can be expressed as

$$\begin{aligned} \text{SER} \approx \sum_{g=1}^{2^{\eta_s}} \frac{1}{2^{\eta_s}} \Bigg[& Q\left(\frac{\left\|\sum_{\mathscr{I}_g} \mathbf{h}_{\mathscr{I}_g}\right\|}{\sqrt{4L_a\sigma_w^2}}\right) + \frac{1}{M(g)} \sum_{m=1}^{M(g)} Q\left(\frac{D_m^g}{\sqrt{4\sigma_w^2}}\right) \\ & - \frac{1}{M(g)} Q\left(\frac{\left\|\sum_{\mathscr{I}_g} \mathbf{h}_{\mathscr{I}_g}\right\|}{\sqrt{4L_a\sigma_w^2}}\right) \sum_{m=1}^{M(g)} Q\left(\frac{D_m^g}{\sqrt{4\sigma_w^2}}\right) \Bigg]. \end{aligned} \tag{2.11}$$

For $U = 1$, the closed-form expression becomes

$$\begin{aligned} \text{SER} \approx \sum_{g=1}^{2^{\eta_s}} \frac{1}{2^{\eta_s}} \Bigg[& Q\left(\frac{\left\|\sum_{\mathscr{I}_g} \mathbf{h}_{\mathscr{I}_g}\right\|}{\sqrt{4L_a\sigma_w^2}}\right) + \frac{1}{M} \sum_{m=1}^{M} Q\left(\frac{D_m^g}{\sqrt{4\sigma_w^2}}\right) \\ & - \frac{1}{M} Q\left(\frac{\left\|\sum_{\mathscr{I}_g} \mathbf{h}_{\mathscr{I}_g}\right\|}{\sqrt{4L_a\sigma_w^2}}\right) \sum_{m=1}^{M} Q\left(\frac{D_m^g}{\sqrt{4\sigma_w^2}}\right) \Bigg]. \end{aligned} \tag{2.12}$$

In FGSM system, the received SNR can be calculated as

$$\gamma = \frac{E_s}{L\sigma_w^2} \sum_{p=1}^{P} \left| \sum_{l=1}^{L} h_{l,p} \right|^2, \tag{2.13}$$

where $h_{l,p}$ represents the entry of the VLC channel matrix $\mathbf{H}$ between l-th LED and p-th PD, $l = 1, \ldots, L$, $p = 1, \ldots, P$. In Eq. (2.13), $\mathbb{E}\left[\|\mathbf{h}_l\|^2\right]$ is a constant, where $\mathbf{h}_l$ is the l-th column of $\mathbf{H}$ and $\mathbb{E}[\cdot]$ refers to the expectation operator.

2.3.2 SER Optimization

The average SER in Eq. (2.11) can be optimized by selecting the appropriate modulation sizes $\mathbf{m} = [M(1) \ldots M(U)]$ given a predefined value of a spectral efficiency η_0. The optimization problem of the average SER can be formulated as

$$\mathbf{m} = \arg \min_{\mathbf{m}=[M(1)\ldots M(U)]} \{\text{SER}|\eta_0\}. \tag{2.14}$$

The optimization problem in Eq. (2.14) is a global one and the objective function is non-convex. Thus, this optimization can be solved by the exhaustive search algorithm [68, Ch. 1]. In our case, the total number of possible sets (i.e., possible sets of the modulation sizes at a given spectral efficiency) is typically low so that exhaustive search can be efficiently employed. If required, for further complexity reduction, we can utilize the concept of variance reduction technique [69, Ch. 6] as detailed below.

Assume that $\mathbf{m}_k = [M_k(1) \ldots M_k(U)]$ defines the k-th possible set of the modulation sizes at a predefined value of the spectral efficiency η_0, where $k = 1, \ldots, K$ and K is the total possible sets.

Step1: Define the value of the spectral efficiency η_0 and all possible sets of the modulation sizes $\mathbf{m}_k$ for $\forall k = 1, \ldots, K$ at η_0.

Step 2: Calculate variance estimate $\text{V}(\mathbf{m}_k)$ of each k-th possible set of the modulation size as

$$\text{V}(\mathbf{m}_k) = \frac{1}{2^{\eta_s}} \sum_{u=1}^{U} N_u \left(M_k(u) - \bar{m}_k\right)^2, \tag{2.15}$$

where $\bar{m}_k$ represents the average of all elements in $\mathbf{m}_k$.

Step 3: Choose $\grave{K}$ sets out of K possible sets of the modulation sizes which have the lowest $\text{V}(\mathbf{m}_k)$ values.

Step 4: Use the chosen $\grave{K}$ sets for Eq. (2.14).

As an example, consider an FGSM system with $L = 8$, $U = 2$ ($N_1 = 2^{\eta_s}/2$, $N_2 = 2^{\eta_s}/2$), and $\eta = 7.5$ bpcu. There are only 6 possible sets of modulation sizes (i.e., $K = 6$). Specifically, for $L_a = 2$, the possible sets are $\mathbf{m}_1 = [2\ 64]$, $\mathbf{m}_2 = [4\ 32]$ and $\mathbf{m}_3 = [8\ 16]$; for $L_a = 3$, the possible sets are $\mathbf{m}_4 = [2\ 16]$ and $\mathbf{m}_5 = [4\ 8]$; for $L_a = 4$, the possible set is $\mathbf{m}_6 = [2\ 4]$. If we now apply variance reduction technique, we have $\text{V}(\mathbf{m}_1) = 961$,

$\mathrm{V}(\mathbf{m}_2) = 196$, $\mathrm{V}(\mathbf{m}_3) = 16$, $\mathrm{V}(\mathbf{m}_4) = 49$, $\mathrm{V}(\mathbf{m}_5) = 4$, and $\mathrm{V}(\mathbf{m}_6) = 1$. If $\grave{K} = 2$, the chosen possible sets are $\mathbf{m}_5 = [4\ 8]$ and $\mathbf{m}_6 = [2\ 4]$. Therefore, the search set of 6 possible solutions are now reduced to 2.

2.4 Decoding Complexity

The decoding complexity can be assessed in terms of the number of additions and multiplications required to decode the transmitted signal at the receiver side [70].

From Eq. (2.3) on page 19, the total number of multiplications and additions of the proposed FGSM system are respectively given as

$$\mathrm{Mul}_{\mathrm{FGSM}} = 2P \sum_{u=1}^{U} N_u M(u), \tag{2.16}$$

$$\mathrm{Add}_{\mathrm{FGSM}} = (2P-1) \sum_{u=1}^{U} N_u M(u) + 2^{\eta_s} P (L_a - 1). \tag{2.17}$$

Note that the extra complexity required for the FGSM over the ASM is $2^{\eta_s} P (L_a - 1)$ additions only (no extra multiplications are required); these extra additions come from activating L_a LEDs. Thus, the total number of multiplications and additions for the ASM are respectively calculated as

$$\mathrm{Mul}_{\mathrm{ASM}} = 2P \sum_{u=1}^{U} N_u M(u), \tag{2.18}$$

$$\mathrm{Add}_{\mathrm{ASM}} = (2P-1) \sum_{u=1}^{U} N_u M(u). \tag{2.19}$$

It is worth noting that multiplications are more decisive in the decoding complexity compared with the additions. Since Eq. (2.16) and Eq. (2.18) are the same, the proposed FGSM provides almost the same decoding complexity as the ASM system.

2.5 *Results and Discussions*

In this section, Monte-Carlo simulations are performed to assess our findings and analysis. An 8×8 VLC channel is used, which is chosen from subsets of the general 16×16 MIMO system developed in [28]. We consider a fixed transmit power for both ASM and proposed FGSM schemes in order to ensure a fair comparison. The channel state information is considered to be perfectly known at the receiver. The normalized channel matrix (i.e., $\mathbb{E}[\|\mathbf{h}_l\|^2]$ is constant for $\forall l = 1, \ldots, L$) for the 8×8 MIMO setup is given by [71]

$$\mathbf{H} = 10^{-6} \times \begin{pmatrix} 0.377 & 0.483 & 0.446 & 0.523 & 0.400 & 0.466 & 0.273 & 0.430 \\ 0.455 & 0.407 & 0.395 & 0.427 & 0.384 & 0.362 & 0.304 & 0.141 \\ 0.236 & 0.243 & 0.300 & 0.136 & 0.356 & 0.384 & 0.388 & 0.382 \\ 0.316 & 0.202 & 0.300 & 0.119 & 0.353 & 0.164 & 0.349 & 0.478 \\ 0.211 & 0.206 & 0.270 & 0.266 & 0.327 & 0.362 & 0.428 & 0.426 \\ 0.240 & 0.224 & 0.285 & 0.343 & 0.304 & 0.338 & 0.426 & 0.450 \\ 0.391 & 0.501 & 0.388 & 0.413 & 0.345 & 0.344 & 0.312 & 0.122 \\ 0.490 & 0.397 & 0.401 & 0.389 & 0.350 & 0.338 & 0.315 & 0.153 \end{pmatrix}. \quad (2.20)$$

Figure 6 on the following page and Figure 7 on page 27 present the average SER performance of the proposed FGSM compared to ASM for $L = 8$ with fixed values of spectral efficiency. Moreover, a comparison with conventional GSM is also included In Figure 6 on the following page, two groups (i.e., $U = 2$) are used ($N_1 = 2^{\eta_s}/2$, $N_2 = 2^{\eta_s}/2$), whereas in Figure 7 on page 27, three groups (i.e., $U = 3$) are utilized ($N_1 = (3/8)\,2^{\eta_s}$, $N_2 = (1/4)\,2^{\eta_s}$, $N_3 = (3/8)\,2^{\eta_s}$). The modulation sizes for both ASM and FGSM are optimized according to the optimization formula given in Eq. (2.14) on page 23.

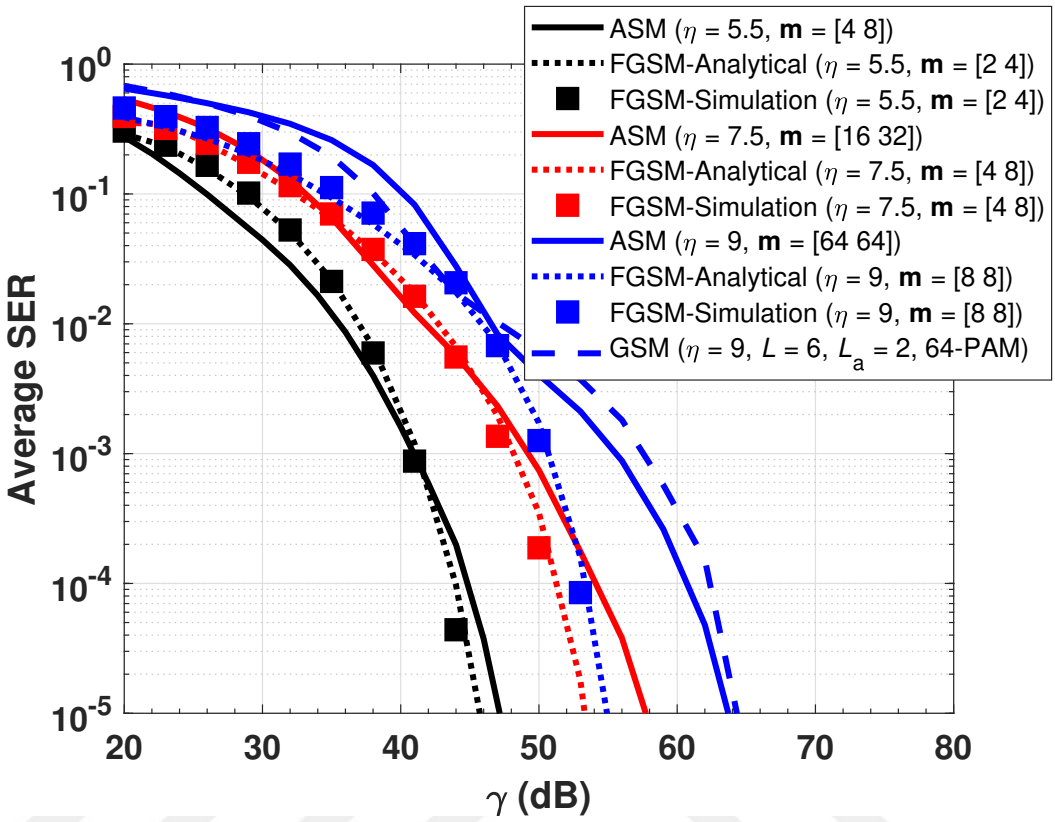

Figure 6: Performance comparison of ASM and FGSM for $L = 8$ and $U = 2$ ($N_1 = \frac{2^{\eta_s}}{2}, N_2 = \frac{2^{\eta_s}}{2}$).

It can be observed from Figure 6 and Figure 7 on the following page that the proposed FGSM obtains better average SER results compared to ASM at the same spectral efficiency. For example, at the SER of 10^{-5} in Figure 6, the required SNR values are 47.2 dB and 57.7 dB for ASM to provide overall spectral efficiencies of 5.5 bpcu and 7.5 bpcu, respectively. Whereas, the required SNR values to provide 5.5 bpcu and 7.5 bpcu are decreased to 45.7 dB and 53.3 dB, respectively, by using the proposed FGSM system. This indicates that the FGSM improves the average SER by 1.5 dB and 4.4 dB for spectral efficiencies of 5.5 bpcu and 7.5 bpcu, respectively. In Figure 7 on the following page, to achieve a spectral efficiency of 8 bpcu at the SER of 10^{-5}, the required SNR is 59.9 dB for ASM while this value decreases to 54.1 dB by using the proposed FGSM. This shows that the FGSM can improve the average SER performance by 5.8 dB for a spectral efficiency of 8 bpcu in

comparison with ASM. Moreover, it is observed that, at the same spectral efficiency, the proposed FGSM achieves a better SER in comparison with both ASM and conventional GSM in Figure 6 on the previous page and Figure 7. For instance, at a spectral efficiency of 9 bpcu, the proposed FGSM scheme enhances the average SER by 9.5 dB in comparison to both ASM and conventional GSM.

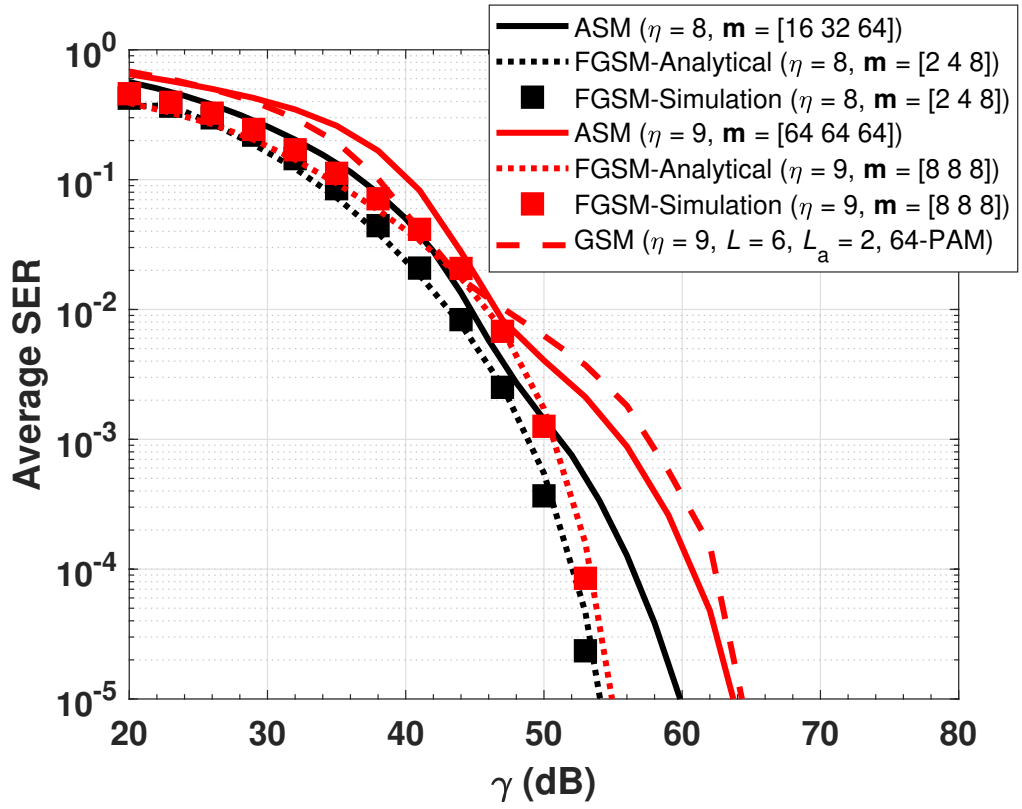

Figure 7: Performance comparison of ASM and FGSM for $L = 8$ and $U = 3$ ($N_1 = \frac{3}{8}2^{\eta_s}$, $N_2 = \frac{1}{4}2^{\eta_s}$, $N_3 = \frac{3}{8}2^{\eta_s}$).

In Figure 8 on the next page and Figure 9 on page 29, we provide a SER comparison for FGSM and ASM schemes with the same modulation sizes and $L = 8$. Figure 8 on the next page represents the performance comparison for $U = 2$ ($N_1 = 2^{\eta_s}/2$, $N_2 = 2^{\eta_s}/2$) and $\mathbf{m} = [4\ 32]$. Figure 9 shows the performance comparison for $U = 3$ ($N_1 = (3/8)\,2^{\eta_s}$, $N_2 = (1/4)\,2^{\eta_s}$, $N_3 = (3/8)\,2^{\eta_s}$) and $\mathbf{m} = [4\ 8\ 32]$. As shown in Figure 8 on the following page and Figure 9 on page 29, while ASM can only provide an overall spectral efficiency

of 6.5 bpcu, the proposed FGSM can improve the overall spectral efficiency by varying the number of active LEDs (L_a). For instance, the FGSM obtains overall spectral efficiency values of 7.5, 8.5 and 9.5 bpcu for $L_a = 2$, 3 and 4, respectively, which results in relative improvements of 15.4%, 30.8% and 46.2%, respectively.

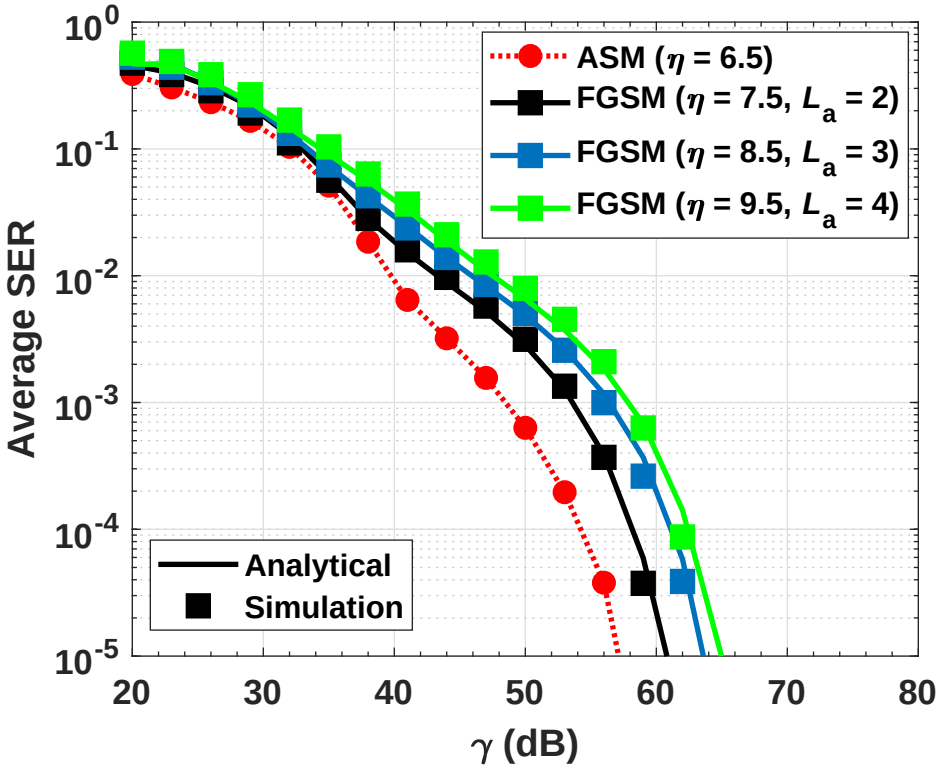

Figure 8: Performance comparison of ASM and FGSM for $\mathbf{m} = [4\ 32]$, $L = 8$ and $U = 2$ $\left(N_1 = \frac{2^{\eta_s}}{2}, N_2 = \frac{2^{\eta_s}}{2}\right)$.

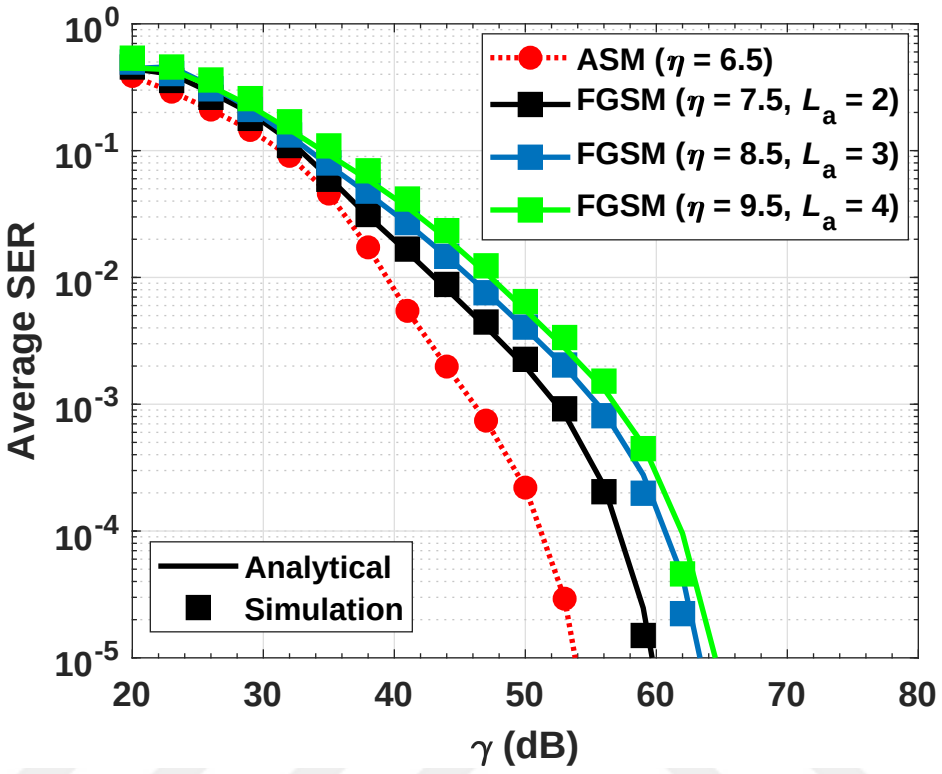

Figure 9: Performance comparison of ASM and FGSM for $\mathbf{m} = [4\ 8\ 32]$, $L = 8$ and $U = 3$ $\left(N_1 = \frac{1}{4}2^{\eta_s}, N_2 = \frac{3}{8}2^{\eta_s}, N_3 = \frac{3}{8}2^{\eta_s}\right)$.

It can be seen from all results that the analytical closed-form expression of the proposed system given in Eq. (2.11) on page 22 provides a close representation of the simulated SER results. In addition to the superiority of the proposed system without almost extra cost in the decoding complexity as indicated in Section 2.4.

CHAPTER III

ADAPTIVE UNIPOLAR MIMO-OFDM FOR VISIBLE LIGHT COMMUNICATIONS

3.1 Introduction

U-OFDM appears as an attractive optical OFDM solution for emerging VLC systems. The U-OFDM scheme is more power-efficient than DCO-OFDM since it does not require a DC bias as DCO-OFDM [6, Ch. 12]. As a result, U-OFDM can achieve a lower BER than DCO-OFDM. In this chapter, we propose an adaptive transmission technique for the MIMO VLC system in conjunction with U-OFDM to exploit the U-OFDM benefits. The proposed adaptive MIMO U-OFDM VLC system is implemented to support three different MIMO modes (RC, SMUX, and SM) that enable a set of different modulation sizes. Depending on the received SNR and target BER, the proposed adaptive transmission system switches between the available MIMO modes and adjusts its modulation size to achieve higher spectral efficiency. The proposed U-OFDM system is applied over different VLC MIMO setups with realistic channel models for 8×8, 4×4 and 2×2 MIMO systems. Our simulation results show that the proposed adaptive system provides a significant spectral efficiency improvement over stand-alone U-OFDM MIMO modes/setups.

The structure of this chapter is as follows: Section 3.2 presents the proposed adaptive MIMO U-OFDM VLC system. In Section 3.3, we describe the adaptive transmission algorithm. Section 3.4 describes the indoor MIMO VLC channel model. In Section 3.5, our numerical results are given.

3.2 System Model

Consider a MIMO system with L LEDs at the transmitter and P PDs at the receiver as shown in Figure 10. The proposed adaptive MIMO system is designed to support three different MIMO modes (i.e., RC, SM, and SMUX). The RC mode is the simplest MIMO mode [7], in which all LEDs simultaneously emit the same signal for achieving diversity gain through repetition (see Figure 11(a) on the following page). In the SMUX mode [72, Ch. 10], independent information signals are transmitted simultaneously from all LEDs to achieve multiplexing gain (see Figure 11(b) on the next page). For the SM mode [73], the transmitter chooses randomly only one of the LEDs as active and the index of the activated LED carries information in addition to the modulated signal transmitted from the selected LED (see Figure 11(c) on the following page). The proposed adaptive system selects the appropriate MIMO mode and modulation size based on the received SNR, then, reports this information to the transmitter through a feedback link.

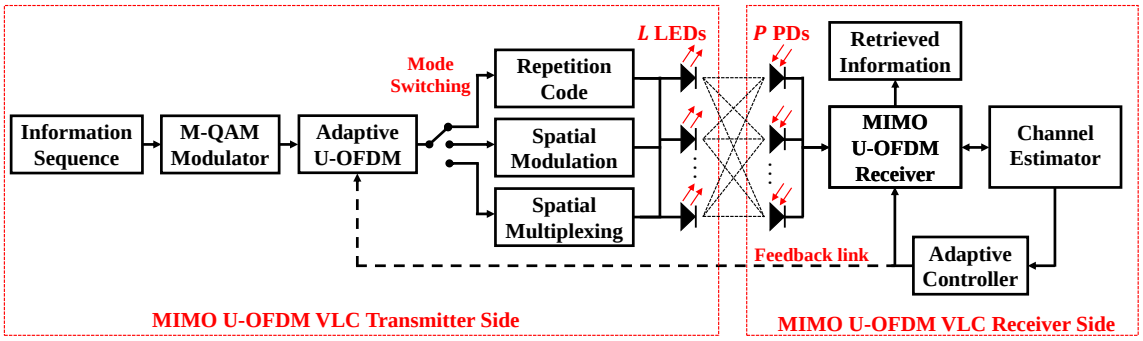

Figure 10: Block diagram of the proposed adaptive MIMO U-OFDM VLC system.

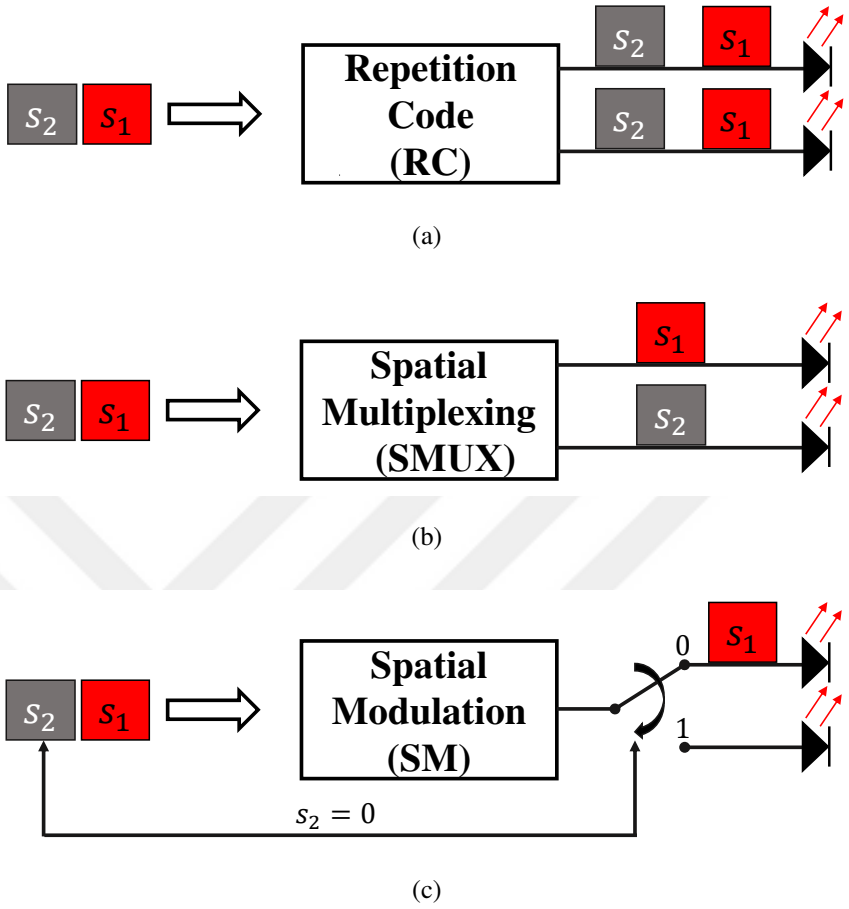

Figure 11: (a) RC, (b) SMUX and (c) SM.

The adaptive system architecture is built on the U-OFDM system. In the U-OFDM system, binary information is first mapped to complex symbols using M-ary QAM with the modulation size M and the average electrical symbol energy E. The complex-valued modulated symbols are applied to Hermitian symmetry before IFFT, for extracting a real-valued bipolar signal. A cyclic prefix with the size of N_{CP} is appended to real-valued bipolar signal in order to overcome the ISI. The resulting real-valued bipolar signal is converted into a unipolar signal by doubling the original OFDM frame. The first OFDM frame refers to the positive samples and the second one represents negative samples. In the first frame, the negative samples set as inactive (i.e., set to zero). In the second frame, the positive samples set as inactive and the negative samples are multiplied by -1 to be

positive. Then, the resulting signal propagates through the optical VLC channel to the PDs. At the receiver side, the negative frame of U-OFDM signal is subtracted from the positive frame. After removing the cyclic prefix, the Fast Fourier Transform (FFT) output at p-th PD, $p = 1,2,\ldots,P$ is given by

$$y_p(n) = \sqrt{\frac{E}{L_a}} \sum_l h_{p,l}(n)\, s_l(n) + w_p(n), \quad n = 1,2,\ldots,N, \tag{3.1}$$

where $y_p(n)$ is the received signal for the n-th subcarrier at the p-th PD and the total number of subcarriers (FFT size) is denoted by N. In Eq. (3.1), $s_l(n)$ represents the transmitted signal from the l-th LED for the n-th subcarrier and drawn from M-QAM constellation. In case of RC and SMUX modes, $l = 1,2,\ldots,L$, where $s_1(n) = s_2(n) = \cdots = s_L(n)$ for RC and $s_1(n), s_2(n), \cdots, s_L(n)$ are independent symbols for SMUX. Whereas in case of the SM mode, $l \in \{1,2,\ldots,L\}$ corresponds to the activated LED index. In Eq. (3.1), L_a is the activated LEDs, where $L_a = L$ in case of the RC and SMUX modes, while $L_a = 1$ for SM mode. Here, $h_{p,l}(n)$ represents the n-th subcarrier VLC channel gain between the p-th PD and the l-th LED, $w_p(n) \sim \mathcal{N}(0, N_0)$ is the AWGN term at the p-th PD with zero mean and variance N_0, and N_0 denotes the noise PSD.

At the receiver side, the ML detector is used for RC, SMUX, and SM. The ML decision for RC and SMUX is given by

$$\hat{\mathbf{s}}(n)^{(\mathrm{ML})} = \arg\min_{\mathbf{s}(n)} \|\mathbf{y}(n) - \mathbf{H}(n)\,\mathbf{s}(n)\|^2, \tag{3.2}$$

where $\mathbf{y}(n)$ is the received U-OFDM signal vector with dimensions $P \times 1$, and each element of this vector is given by $y_p(n)$ that is defined earlier in Eq. (3.1). In Eq. (4.10), $\mathbf{s}(n) = \begin{bmatrix} s_1(n) & s_2(n) & \ldots & s_L(n) \end{bmatrix}^{\mathrm{T}}$ is the transmitted U-OFDM signal vector with dimensions $L \times 1$, and $[\cdot]^{\mathrm{T}}$ denotes the transpose. Here, $\mathbf{H}(n)$ denotes the MIMO channel gains matrix with dimensions $P \times L$, where each matrix entry is defined by $h_{p,l}(n)$.

For the SM mode, the ML decision should be modified where the search is over both LED index and modulated signal as

$$\left[\hat{l}^{(\mathrm{ML})}, \hat{s}(n)^{(\mathrm{ML})}\right] = \underset{\substack{s(n) \\ l\in\{1,2,\ldots L\}}}{\arg\min} \|\mathbf{y}(n) - \mathbf{h}_l(n)\, s(n)\|^2 . \tag{3.3}$$

where $\mathbf{h}_l(n)$ is the l-th column of $\mathbf{H}(n)$. The ML detector of SMUX might be prohibitive for higher modulation sizes or larger MIMO setups due to its high complexity [70]. As a result, the ZF equalizer is used for an alternative with lower detection cost. The ZF decision expressed as

$$\hat{\mathbf{s}}(n)^{(\mathrm{ZF})} = \left((\mathbf{H}(n))^{\mathrm{T}}\mathbf{H}(n)\right)^{-1}\left((\mathbf{H}(n))^{\mathrm{T}}\mathbf{y}(n)\right). \tag{3.4}$$

For further performance improvement, the Optimal Ordering Successive Interference Cancellation (OSIC) is adopted after ZF equalization as described in [72, Sec. (11.2)].

3.3 *Adaptive Transmission Technique*

The proposed adaptive transmission technique for MIMO U-OFDM VLC system is described. The basic idea of adaptive transmission is to switch the transmission parameters, such as MIMO modes or/and MIMO setups, based on the received SNR and a target BER, P_{th}. A feedback link is required for transferring the necessary information to the transmitter. VLC system usually employs the RF, or infrared waves as a feedback link [74]. Thus, the feedback link does not provide additional overhead to the VLC system. The steps of the adaptive transmission technique are described as follows:

Step 1: Define threshold BER value P_{th} for given E and $\mathbf{H}$. Here, $\mathbf{H} = \mathbf{H}(n) \in \mathbb{R}^{P\times L}$ for $\forall\, n$ and $\mathrm{E}[\|\mathbf{h}_l\|^2]$ is constant, where $l = 1, 2, \ldots, L$ and $\mathrm{E}[\cdot]$ denotes the expectation operator.

Step 2: Calculate the received SNR, γ, as

$$\gamma = \frac{E}{LN_0}\sum_{p=1}^{P}\left|\sum_{l=1}^{L} h_{p,l}\right|^2 . \tag{3.5}$$

The Eq. (3.5) is valid for all MIMO modes, $\Xi \in \{\mathrm{RC,SM,SMUX}\}$, based on $\mathbf{H}$ that will be defined in Section 3.4 on the next page.

Step 3: Find the maximum constellation size $M_{\Xi}^{(\max)}$, which satisfies P_{th}. Then, calculate the corresponding spectral efficiency for each MIMO mode, η_{Ξ}, in Bits per Second per Hertz (b/s/Hz) as [6, Ch. 12]

$$\eta_{\text{RC}} = \frac{1}{2}\left(\frac{N/2-1}{N+N_{\text{CP}}}\right)\log_2\left(M_{\text{RC}}^{(\max)}\right), \tag{3.6}$$

$$\eta_{\text{SM}} = \frac{1}{2}\left(\frac{N/2-1}{N+N_{\text{CP}}}\right)\log_2\left(N_t M_{\text{SM}}^{(\max)}\right), \tag{3.7}$$

$$\eta_{\text{SMUX}} = \frac{N_t}{2}\left(\frac{N/2-1}{N+N_{\text{CP}}}\right)\log_2\left(M_{\text{SMUX}}^{(\max)}\right). \tag{3.8}$$

Step 4: Find the maximum spectral efficiency resulted from (3.6)-(3.8) and determine its mode, $\Xi^{(\max)}$. Then, the adaptive transmission technique switches the operation mode to $\Xi^{(\max)}$. Our adaptive transmission technique is summarized in Algorithm 1.

Algorithm 1 Pseudo-code of adaptive transmission technique.

1. **Given** P_{th}, $\mathbf{H}$ and E.
2. **Calculate** γ from (3.5).
3. **For** $\Xi \in \{\text{RC,SM,SMUX}\}$, **do**
4. **Find** $M_{\Xi}^{(\max)}$ which BER $\left(M_{\Xi}^{(\max)}\right) \leq P_{\text{th}}$.
5. **Calculate** $\eta_{\Xi}\left(M_{\Xi}^{(\max)}\right)$ using (3.6)-(3.8).
6. **End**
7. **Find** $\Xi^{(\max)}$ corresponds to maximum $\eta_{\Xi}\left(M_{\Xi}^{(\max)}\right)$, $\forall\ \Xi$.
8. **Switch** operating mode to $\Xi^{(\max)}$.

3.4 Indoor MIMO VLC Channel

In this chapter, the MIMO setups of 8×8, 4×4 and 2×2 are considered. The indoor VLC channels developed in [28] are used for our simulations. The considered MIMO setups are chosen from subsets of the general 16×16 MIMO system in [28]. The normalized channel

matrices (i.e., $\mathrm{E}[\|\mathbf{h}_l\|^2]$ is fixed for all $l = 1,2,\ldots,L$) for 8×8, 4×4 and 2×2 MIMO setups are respectively given by

$$\mathbf{H} = 10^{-6}\times \begin{pmatrix} 0.377 & 0.483 & 0.446 & 0.523 & 0.400 & 0.466 & 0.273 & 0.430 \\ 0.455 & 0.407 & 0.395 & 0.427 & 0.384 & 0.362 & 0.304 & 0.141 \\ 0.236 & 0.243 & 0.300 & 0.136 & 0.356 & 0.384 & 0.388 & 0.382 \\ 0.316 & 0.202 & 0.300 & 0.119 & 0.353 & 0.164 & 0.349 & 0.478 \\ 0.211 & 0.206 & 0.270 & 0.266 & 0.327 & 0.362 & 0.428 & 0.426 \\ 0.240 & 0.224 & 0.285 & 0.343 & 0.304 & 0.338 & 0.426 & 0.450 \\ 0.391 & 0.501 & 0.388 & 0.413 & 0.345 & 0.344 & 0.312 & 0.122 \\ 0.490 & 0.397 & 0.401 & 0.389 & 0.350 & 0.338 & 0.315 & 0.153 \end{pmatrix}, \tag{3.9}$$

$$\mathbf{H} = 10^{-6}\times \begin{pmatrix} 0.5356 & 0.6831 & 0.3838 & 0.5762 \\ 0.3354 & 0.3440 & 0.5461 & 0.5121 \\ 0.3414 & 0.3161 & 0.5987 & 0.6031 \\ 0.6958 & 0.5614 & 0.4428 & 0.2052 \end{pmatrix}, \tag{3.10}$$

$$\mathbf{H} = 10^{-6}\times \begin{pmatrix} 0.6958 & 0.7644 \\ 0.7182 & 0.6447 \end{pmatrix}. \tag{3.11}$$

3.5 *Results and Discussions*

In this section, the spectral efficiency and date rate of the proposed adaptive U-OFDM MIMO VLC system are evaluated for different MIMO setups mentioned in Section 3.4. The data rate equals $\eta \times B$ Bits per Second (b/s), where B is the system bandwidth. From Figure 13 on page 39 to Figure 16 on page 42, the left and right vertical axis represent the spectral efficiency and data rate, respectively; while the horizontal axis represents γ given from Eq. (3.5). The channel state information is assumed to be perfectly known at the receiver side. The ML detector is used for simulating the BER performances of RC and

SM MIMO modes for all modulation sizes. Whereas the simulation of BER performance for the SMUX MIMO mode utilizes three different detectors (ML, ZF, and ZF-OSIC) according to the complexity. For fair comparison, we consider fixed transmit power for all modes. The simulation parameters are provided in Table 2.

Table 2: Simulation parameters.

Parameters	Symbol	Value
FFT size	N	1024 [5]
Cyclic prefix size	N_{CP}	4 [5]
Target BER	P_{th}	10^{-6}
System bandwidth	B	20 MHz [5]
Available modulation sizes	M	4 to 4096
MIMO setup	$N_r \times N_t$	2×2, 4×4 and 8×8

Figure 12 on the following page depicts the BER performance for different modes of the 8×8 MIMO-VLC system utilizing U-OFDM. The proposed adaptive transmission technique uses these BER results to find $M_{\Xi}^{(\max)}$ that satisfies P_{th} for $\forall\ \Xi$. For instance, at $\gamma = 60$ dB and $P_{\text{th}} = 10^{-6}$, the maximum constellation size for the RC mode is 4096 and provides 2.9825 b/s/Hz (i.e., $M_{\text{RC}}^{(\max)} = 4096$ and $\eta_{\text{RC}} = 2.9825$ b/s/Hz). Whereas for SM the mode, $M_{\text{SM}}^{(\max)} = 32$ and $\eta_{\text{SM}} = 1.9883$ b/s/Hz. In the SMUX mode, there is no $M_{\text{SMUX}}^{(\max)}$ that satisfies P_{th}. Therefore, at $\gamma = 60$ dB, the proposed algorithm selects the RC mode as the operation mode. It should be noted that in a real system, the proposed algorithm switches between the modes/setups and uses the theoretical equations instead of the BER curves.

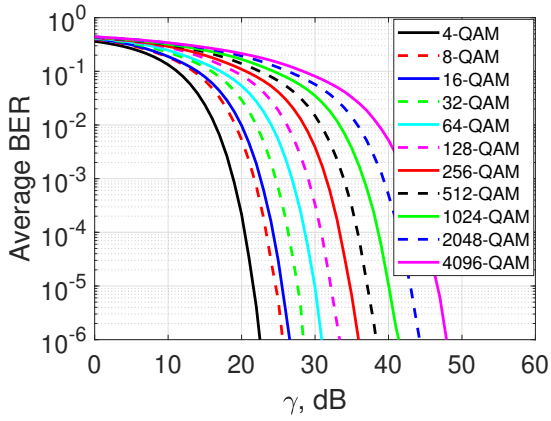

(a)

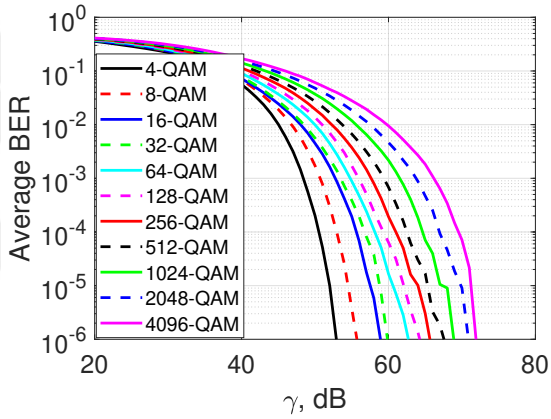

(b)

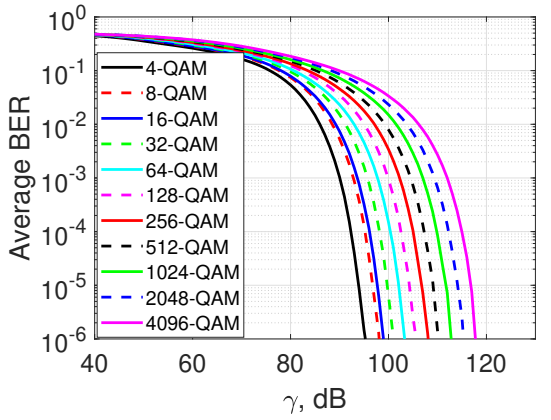

(c)

Figure 12: BERs performances for U-OFDM VLC system of 8×8 MIMO modes (a) RC, (b) SM, and (c) SMUX.

In Figure 13, the spectral efficiency and the corresponding data rate of the proposed adaptive transmission system (indicated by dotted line) are depicted for the 8×8 MIMO U-OFDM VLC system. For this setup, the ZF equalizer is employed for the SMUX in all modulation sizes. As benchmarks, the stand-alone RC, SM and SMUX systems are considered. It is observed from Figure 13 that in the low SNR region, RC outperforms both SM and SMUX as a result of diversity gains. Specifically, the adaptive system selects the RC mode when $\gamma < 68$ dB. In the ranges of 68 dB to 95 dB, the adaptive system selects the SM mode. After 95 dB, the SMUX significantly outperforms its counterparts by taking advantage of multiplexing gains and is therefore selected as the operation mode. It should be noted that the spectral efficiencies of the RC and SM saturate respectively at 48 dB and 75 dB, where 4096-QAM is employed. The maximum achievable spectral efficiency for the RC and SM are respectively 2.982 and 3.728 b/s/Hz which respectively correspond to data rates of 59.64 and 74.56 Megabits per Second (Mb/s). The SMUX saturates at 118 dB and the achievable maximum spectral efficiency of 23.86 b/s/Hz corresponds to a data rate of 477.2 Mb/s.

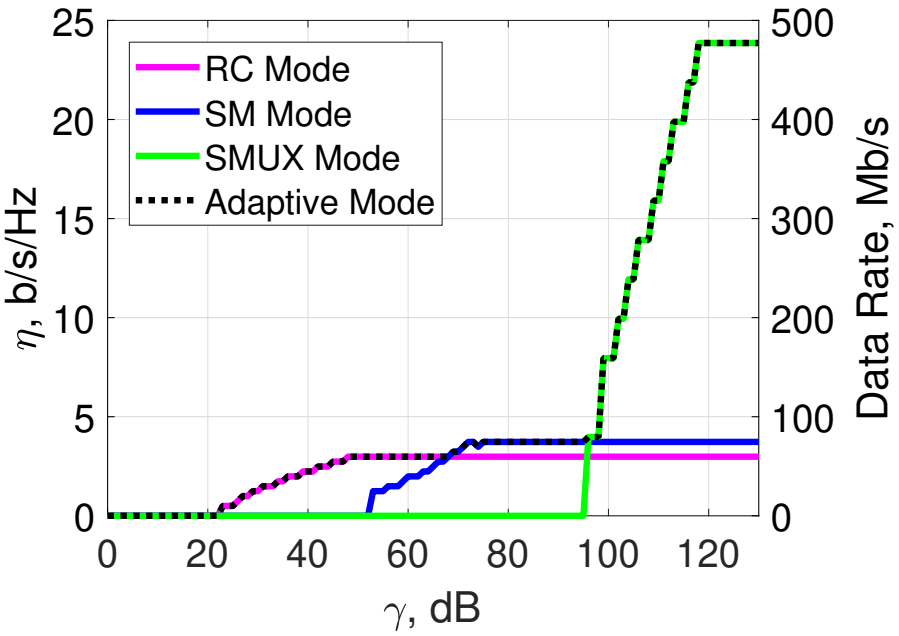

Figure 13: Spectral efficiency and date rate for 8×8 MIMO U-OFDM VLC system.

Figure 14 and Figure 15 on the following page show the spectral efficiency and the corresponding data rate of 4×4 and 2×2 MIMO U-OFDM VLC systems, respectively. The SMUX uses the ML detector for low modulation sizes (below $M = 128$ and 16 in 2×2 and 4×4 MIMO setups, respectively) and ZF-OSIC detector for the high modulation sizes. In Figure 14, the proposed adaptive transmission system selects the RC mode for $\gamma < 64$ dB as the operation mode. The SM mode is chosen in the range of 64 dB to 73 dB. For $\gamma > 73$ dB, the adaptive transmission system selects the SMUX mode. The maximum achievable spectral efficiency and corresponding data rate for the 4×4 system in Figure 14 decrease to half in comparison with the 8×8 system in Figure 13 on the previous page. In Figure 15 on the following page, the adaptive transmission system chooses the RC mode for $\gamma < 54$ dB. The proposed adaptive transmission system chooses the SMUX mode when $\gamma > 54$ dB. In the 2×2 system (Figure 15 on the next page), the maximum achievable spectral efficiency reduces from 23.86 to 5.965 b/s/Hz and corresponding data rate decreases from 477.2 to 119.3 Mb/s, compared to 8×8 MIMO system.

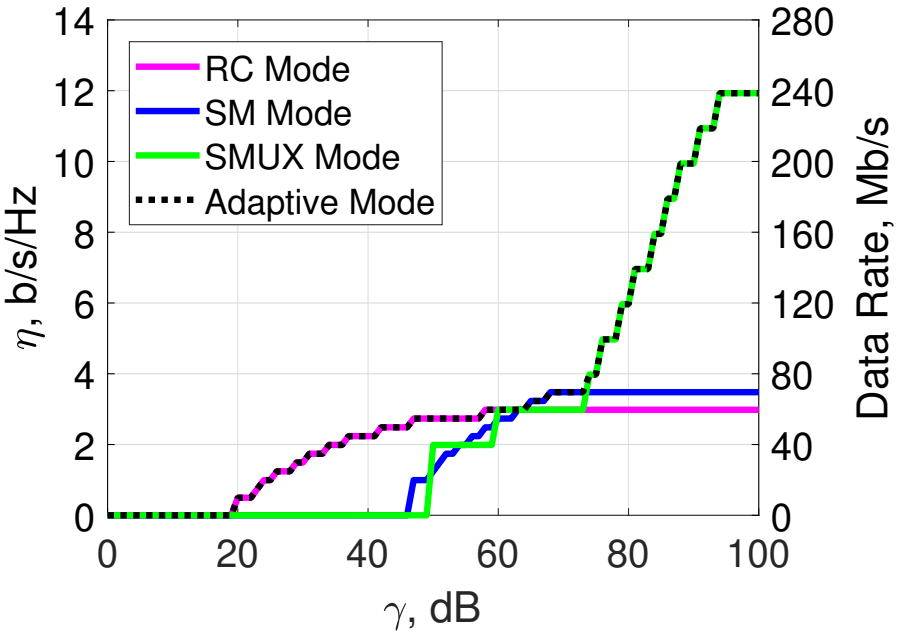

Figure 14: Spectral efficiency and date rate for 4×4 MIMO U-OFDM VLC system.

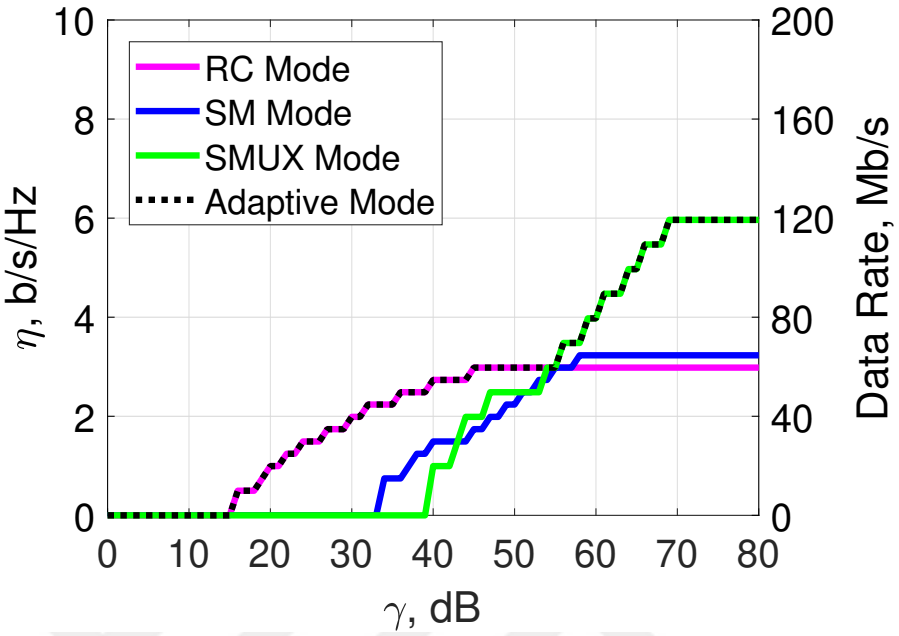

Figure 15: Spectral efficiency and date rate for 2×2 MIMO U-OFDM VLC system.

For further spectral efficiency improvement, switching between the MIMO system setups of 2×2, 4×4 and 8×8 is investigated in Figure 16 on the following page. The proposed adaptive transmission system selects the 2×2 MIMO setup when $\gamma < 79$ dB which achieves 5.965 b/s/Hz with a data rate of 119.3 Mb/s. When γ lies between 79 dB and 104 dB, the adaptive transmission system chooses the 4×4 MIMO setup and the achievable spectral efficiency is 11.93 b/s/Hz with a data rate of 238.6 Mb/s. Finally, the proposed adaptive transmission system activated the 8×8 MIMO setup at $\gamma > 104$ dB, which provides the maximum spectral efficiency and data rate as 23.86 b/s/Hz and 477.2 Mb/s, respectively.

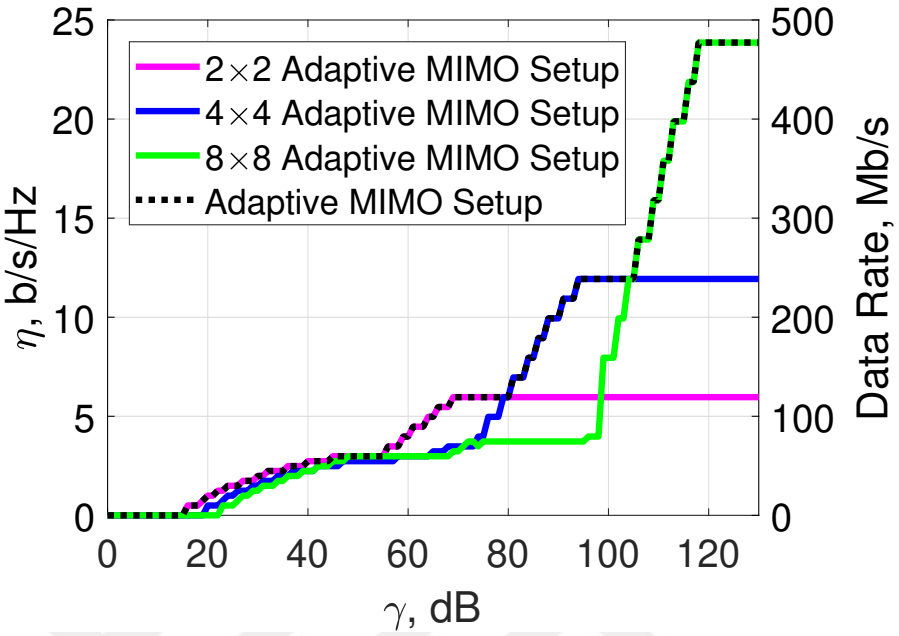

Figure 16: Spectral efficiency and date rate of the adaptive setup technique for MIMO U-OFDM VLC system.

It can be observed from these figures that the proposed adaptive transmission system benefits from RC, SM, and SMUX by employing mode switching relying on the received SNR. Consequently, the proposed adaptive MIMO U-OFDM VLC system exhibits a superior spectral efficiency over the stand-alone modes/setups.

CHAPTER IV

MAGNITUDE AND WRAP-PHASE OFDM FOR MIMO VISIBLE LIGHT COMMUNICATION SYSTEMS

4.1 Introduction

GLIM-OFDM appears as an attractive MIMO OFDM scheme for emerging VLC systems. In this chapter, we propose the so-called MW-OFDM scheme for MIMO VLC systems as well as we derive the ML estimator for the proposed scheme. The proposed MW-OFDM decreases the restriction on the number of LEDs and achieves better BER performance, compared to conventional GLIM-OFDM. This can be done by exploiting the conversion of the complex symbol into a polar form with the magnitudes and wrap-phases. As a result, the proposed MW-OFDM scheme requires a half number of LEDs in a comparison with the conventional GLIM-OFDM. Furthermore, the proposed MW-OFDM scheme provides a significant reduction in the decoding complexity, compared to the conventional GLIM-OFDM. Numerical results are presented over realistic MIMO VLC channels to emphasize the findings of our proposed scheme.

The rest of this chapter is organized as follows: Section 4.2 presents the system model for the proposed MW-OFDM scheme. In Section 4.3, we derive the ML estimator for the proposed MW-OFDM. In Section 4.4, the decoding complexity analysis for the proposed MW-OFDM is perform in a comparison with the conventional GLIM-OFDM schemes. Section 4.5 presents numerical results to evaluate and demonstrate the superiority of our proposed MW-OFDM scheme, compared to the existing ones.

4.2 System Model

The block diagram of the proposed MW-OFDM scheme for a $P \times L$ MIMO VLC system is presented in Figure 17, where P and L are the number of PDs at the receiver and LEDs at the transmitter, respectively. In the proposed MW-OFDM scheme, $N \log_2(M)$ information bit-stream is modulated using M-ary QAM, where N represents the number of the OFDM subcarriers and M is the modulation size. Subsequently, the modulated symbol is directly processed by the IFFT operation without using the Hermitian symmetry. After Parallel-To-Serial (P/S) operation, each complex OFDM sample resulted from IFFT, x_k (where $k = 0, \ldots, N-1$), is converted into polar form with a magnitude, $x_{k,r} = |x_k|$, and a wrap-phase, $x_{k,\theta} = \arg(x_k) \in [0, 2\pi]$. Then, the resultant magnitude and wrap-phase of each OFDM sample are transmitted simultaneously through LEDs.

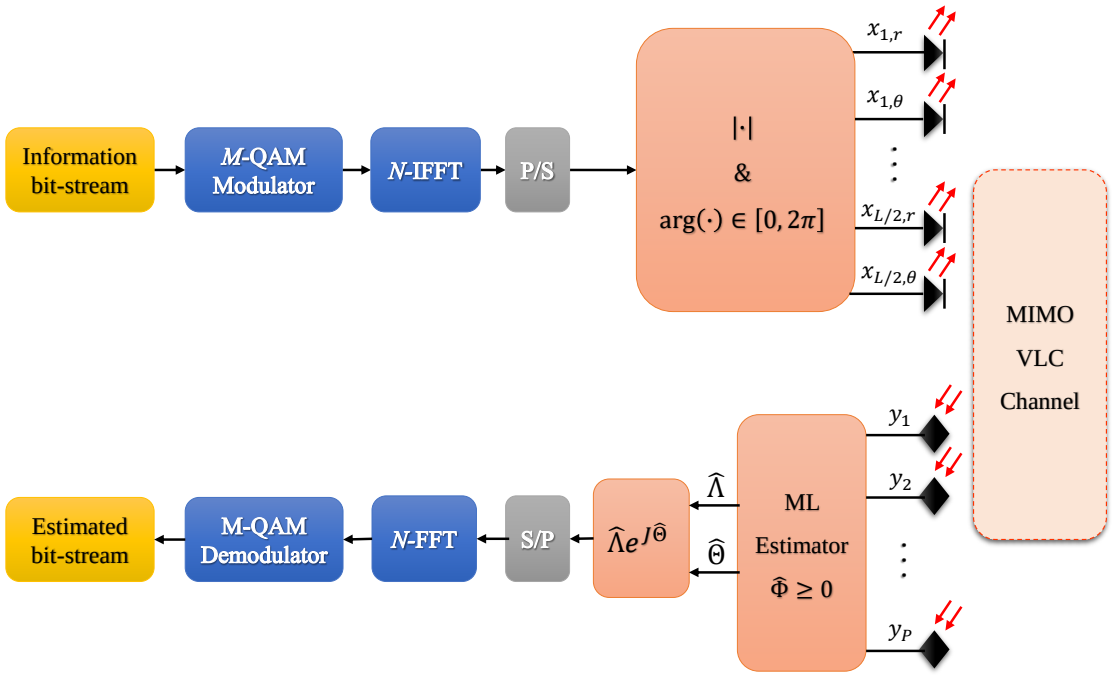

Figure 17: Block diagram of the proposed MW-OFDM for MIMO VLC system

The received signal, $\mathbf{y} = [y_1, \ldots, y_P]^{\mathrm{T}} \in \mathbb{R}^{P \times 1}$, over $P \times L$ MIMO VLC channel is

$$\mathbf{y} = \mathbf{H}\mathbf{x} + \mathbf{w}, \tag{4.1}$$

where $\mathbf{H} = [\mathbf{h}_1, \ldots, \mathbf{h}_L] \in \mathbb{R}^{P\times L}$ is the MIMO VLC channel matrix and $\mathbf{h}_l$ is the l-th column of $\mathbf{H}$, $l = 1, \ldots, L$. Here, $\mathbf{x} = [x_{1,r}, x_{1,\theta}, \ldots, x_{L/2,r}, x_{L/2,\theta}]^{\mathrm{T}} \in \mathbb{R}^{L\times 1}$ is the transmitted vector with magnitudes of $x_{i,r}$ and wrap-phases of $x_{i,\theta}$ for the OFDM samples for $i = 1, \ldots, L/2$, and $[\cdot]^{\mathrm{T}}$denotes the transpose operation. In Eq. (4.1), $\mathbf{w} \in \mathbb{R}^{P\times 1}$ represents the vector of real-valued AWGN samples and each element has zero-mean and variance of σ_w^2. Therefore, Eq. (4.1) can be rewritten as

$$\mathbf{y} = \mathbf{h}_1 x_{1,r} + \mathbf{h}_2 x_{1,\theta} + \ldots + \mathbf{h}_{L-1} x_{L/2,r} + \mathbf{h}_L x_{L/2,\theta} + \mathbf{w}$$

$$= \sum_{i=1}^{L/2} \left(\mathbf{h}_{2i-1} x_{i,r} + \mathbf{h}_{2i} x_{i,\theta}\right) + \mathbf{w}. \tag{4.2}$$

Assume that the k-th complex OFDM sample is $x_k = -1.5 + j2$ for $L = 2$. For the proposed MW-OFDM scheme, x_k is converted into a polar form with a magnitude of $x_{k,r} = 2.5$ and a wrap-phase of $x_{k,\theta} = 2.2143$ rad. Therefore, the transmitted vector is $\mathbf{x} = [2.5 \quad 2.2143]^{\mathrm{T}}$. On the other hand, the transmitted vector for the conventional GLIM-OFDM is $\mathbf{x} = [0 \quad 1.5 \quad 2 \quad 0]^{\mathrm{T}}$. Consequently, the proposed scheme achieves spectral efficiency of $\log_2(M)$ bpcu with a half number of LEDs, compared to the conventional GLIM-OFDM.

The average electrical SNR at the receiver side for the proposed MW-OFDM scheme is denoted by γ and can be calculated as [64, 65]

$$\gamma = \frac{1}{\sigma_w^2} \xi \left(\frac{1}{P} \sum_{p=1}^{P} \sum_{l=1}^{L} h_{p,l} I \right)^2, \tag{4.3}$$

where ξ denotes the electrical-to-optical conversion factor that is taken as a unity, I represents the mean optical intensity that is emitted from the LEDs. The M-QAM constellation is assumed to be normalized in order to have unit-energy symbols [65]. In Eq. (4.3), $h_{p,l}$ represents the channel gain of the VLC wireless link between p-th PD and l-th LED, where $l = 1, \ldots, L$ and $p = 1, \ldots, P$.

It should be noted that the magnitudes and wrap-phases are assumed to follow the Rayleigh distribution and uniform distribution, respectively. Consequently, the average value of I in Eq. (4.3) can be obtained as

$$I = \frac{\mathbb{E}\left[x_{k,r}\right] + \mathbb{E}\left[x_{k,\theta}\right]}{2}, \tag{4.4}$$

where $\mathbb{E}[\cdot]$ denotes the expectation operator. Thus, the average value of I is

$$\begin{aligned} I &= \frac{1}{2}\left[\int_0^{\infty} x_r^2 \exp\left(-\frac{x_r^2}{2}\right) dx_r + \frac{1}{2\pi}\int_0^{2\pi} x_\theta dx_\theta\right] \\ &= \frac{1}{2}\left(\sqrt{\frac{\pi}{2}} + \pi\right). \end{aligned} \tag{4.5}$$

To ensure that the magnitudes and wrap-phases of the OFDM samples stay within the dynamic range of the LEDs, $x_{k,r}$ and $x_{k,\theta}$ are scaled as follows [60]

$$x_{k,r}^s = s_1 x_{k,r}, \qquad x_{k,\theta}^s = s_2 x_{k,\theta}, \tag{4.6}$$

where $x_{k,r}^s$ and $x_{k,\theta}^s$ are the scaled values of $x_{k,r}$ and $x_{k,\theta}$, respectively. Here, s_1 and s_2 are the magnitude and wrap-phase scaling factors, respectively, and expressed as

$$s_1 = \frac{I_{\max} - I_{\min}}{\max\left\{x_{k,r}\right\}}, \qquad s_2 = \frac{I_{\max} - I_{\min}}{\max\left\{x_{k,\theta}\right\}}, \tag{4.7}$$

where $I_{\max}$ and $I_{\min}$ define the maximum and minimum LED current, respectively. Thus, after normalization, the value of I in Eq. (4.3) becomes

$$I = \frac{1}{2}\left(s_1\sqrt{\frac{\pi}{2}} + s_2\pi\right). \tag{4.8}$$

4.3 ML Estimator

In this section, the ML estimator is derived for the proposed MW-OFDM scheme. Let $\Lambda = [x_{1,r}, \ldots, x_{L/2,r}]^{\mathrm{T}}$ define the set of magnitudes of the transmitted OFDM samples, while

$\Theta = [x_{1,\theta}, \ldots, x_{L/2,\theta}]^{\mathrm{T}}$ representing the set of wrap-phases for the transmitted OFDM samples. Consequently, Eq. (4.2) can be rewritten as

$$\mathbf{y} = \mathbf{H}_r \Lambda + \mathbf{H}_\theta \Theta + \mathbf{w}, \tag{4.9}$$

where $\mathbf{H}_r$ and $\mathbf{H}_\theta$ are the odd and even columns of $\mathbf{H}$, respectively. Therefore, the ML estimator for Λ and Θ can be obtained as

$$\left\{\hat{\Lambda}, \hat{\Theta}\right\} = \arg \max_{\Lambda, \Theta} p\left(\mathbf{y} \,|\Lambda, \Theta\right), \tag{4.10}$$

where $p(\mathbf{y}\,|\Lambda, \Theta)$ is the PDF of $\mathbf{y}$, given Λ and Θ, and considering that Λ and Θ are independent. Since the PDF of $\mathbf{y}$ given Λ and Θ is $\mathcal{N}(\mathbf{H}_r\Lambda + \mathbf{H}_\theta\Theta, \sigma_w^2)$, and after simple manipulations, the ML estimator in Eq. (4.10) becomes

$$\left\{\hat{\Lambda}, \hat{\Theta}\right\} = \arg \min_{\Lambda, \Theta} \mathscr{M}^{\mathrm{ML}}\left(\Lambda, \Theta\right), \tag{4.11}$$

where $\mathscr{M}^{\mathrm{ML}}(\Lambda, \Theta)$ is the ML estimator metric that is defined as

$$\mathscr{M}^{\mathrm{ML}}\left(\Lambda, \Theta\right) = \left\|\mathbf{y} - \mathbf{H}_r \Lambda + \mathbf{H}_\theta \Theta\right\|^2. \tag{4.12}$$

Using $\|\mathbf{a}\|^2 = \mathbf{a}^{\mathrm{T}}\mathbf{a}$, Eq. (4.12) becomes

$$\mathscr{M}^{\mathrm{ML}}\left(\Lambda, \Theta\right) = \mathbf{y}^{\mathrm{T}}\mathbf{y} + \Lambda^{\mathrm{T}}\mathbf{H}_r^{\mathrm{T}}\mathbf{H}_r\Lambda + \Theta^{\mathrm{T}}\mathbf{H}_\theta^{\mathrm{T}}\mathbf{H}_\theta\Theta + 2\Lambda^{\mathrm{T}}\mathbf{H}_r^{\mathrm{T}}\mathbf{H}_\theta\Theta - 2\mathbf{y}^{\mathrm{T}}\mathbf{H}_r\Lambda - 2\mathbf{y}^{\mathrm{T}}\mathbf{H}_\theta\Theta. \tag{4.13}$$

Taking the derivative of $\mathscr{M}^{\mathrm{ML}}(\Lambda, \Theta)$ in Eq. (4.13) with respect to Λ and Θ and setting the results to zero, the ML estimator can be formulated as

$$\hat{\mathbf{x}} = \left[\mathbf{A}^{-1}\mathbf{b}\right]^{+}, \tag{4.14}$$

where $[x]^{+} := \max([0, x])$ and $\hat{\mathbf{x}} = [\hat{\Lambda}\ \ \hat{\Theta}]^{\mathrm{T}}$ is the vector of estimated magnitudes and wrap-phases. In Eq. (4.14), and $\mathbf{A}$ and $\mathbf{b}$ are calculated as

$$\mathbf{A} = \begin{bmatrix} \mathbf{H}_r^{\mathrm{T}}\mathbf{H}_r & \mathbf{H}_r^{\mathrm{T}}\mathbf{H}_\theta \\ \mathbf{H}_\theta^{\mathrm{T}}\mathbf{H}_r & \mathbf{H}_\theta^{\mathrm{T}}\mathbf{H}_\theta \end{bmatrix}, \ \mathbf{b} = \begin{bmatrix} \mathbf{H}_r^{\mathrm{T}}\mathbf{y} & \mathbf{H}_\theta^{\mathrm{T}}\mathbf{y} \end{bmatrix}^{\mathrm{T}}. \tag{4.15}$$

After this point, the estimated magnitudes $\hat{\Lambda}$ and wrap-phases $\hat{\Theta}$ are converted into complex samples as $\hat{\Lambda}\exp(J\hat{\Theta})$. Subsequently, the classical steps of the OFDM, such as the Serial-To-Parallel (S/P), FFT operations and M-QAM demodulator are proceed to obtain the estimated information bit-stream.

4.4 *Decoding Complexity*

In this section, the decoding complexity of the conventional GLIM-OFDM schemes in [64–66] is compared to the proposed MW-OFDM scheme. The decoding complexity can be measured by the required number of real additions and real multiplications [65]. In our complexity analysis, the subtraction and division operations are respectively considered as equivalent to addition and multiplication operations.

For the conventional 4×4 GLIM-OFDM in [64, 65], the overall real multiplications and additions are respectively calculated as

$$\mathrm{Mul}_{4\times4\ \mathrm{GLIM}} = (24P+68)N, \tag{4.16}$$

$$\mathrm{Add}_{4\times4\ \mathrm{GLIM}} = 24PN. \tag{4.17}$$

The overall required operations for the 8×8 GLIM-OFDM in [66] are respectively expressed as

$$\mathrm{Mul}_{8\times8\ \mathrm{GLIM}} = (656P+594)N, \tag{4.18}$$

$$\mathrm{Add}_{8\times8\ \mathrm{GLIM}} = (592P+304)N. \tag{4.19}$$

For the proposed MW-OFDM, the cost of forming $\mathbf{A}$ and $\mathbf{b}$ in (4.15) for N OFDM subcarriers requires $P(L^2+L)N$ real multiplications and $(P-1)(L^2+L)N$ real additions. For solving an $L \times L$ linear system equation utilizing the Gauss elimination, the required operations of real multiplications and additions are $(L^3+3L^2-L)/3$ and $(3L^3+3L^2-5L)/6$, respectively [75]. Consequently, the overall real multiplications and additions for $P \times L$ MW-OFDM in Eq. (4.14) can be respectively given as

$$\mathrm{Mul}_{\mathrm{MW}} = \frac{1}{3}L^3N + (P+1)L^2N + \left(P - \frac{1}{3}\right)LN, \tag{4.20}$$

$$\mathrm{Add}_{\mathrm{MW}} = \frac{1}{3}L^3N + \left(P - \frac{1}{2}\right)L^2N + \left(P - \frac{11}{6}\right)LN. \tag{4.21}$$

To see the saving in the decoding complexity of the proposed MW-OFDM over the existing ones, we determine the reduction ratio of the decoding complexity, Γ, as

$$\Gamma = \frac{|C_{\Xi} - C_{\mathrm{MW}}|}{C_{\Xi}}\%, \tag{4.22}$$

where C_{MW} represents the decoding complexity (i.e., multiplications or additions) of the proposed MW-OFDM scheme, and C_{Ξ} denotes the decoding complexity of the compared scheme with $\Xi \in \{4\times4$ GLIM-OFDM [64,65], 8×8 GLIM-OFDM [66]$\}$ using Eq. (4.16)-Eq. (4.21). For example, consider $P=4$ and $L=2$ for the proposed MW-OFDM, the average reduction ratio in the decoding complexity by using the proposed scheme compared to 4×4 GLIM-OFDM in [64,65] is about $\Gamma = 80\%$, whereas $\Gamma = 96\%$ using the proposed scheme with $P=8$ and $L=4$ in a comparison with 8×8 GLIM-OFDM in [66].

4.5 Numerical Results and Discussions

In this section, BER performance comparisons of the proposed MW-OFDM scheme using the ML estimator given in Eq. (4.14) and conventional GLIM-OFDM schemes using the MAP estimator are provided with respect to the average received SNR given in Eq. (4.3).

BER results comparisons versus the average received SNR are presented for different spectral efficiencies in bpcu over realistic MIMO VLC channels. The number of the FFT subcarriers is considered as $N = 256$ [65] and the channel state information is assumed to be perfectly known at the receiver side. To ensure a fair comparison, a fixed transmit power is considered for the proposed MW-OFDM and conventional GLIM-OFDM schemes. In other words, the average value of the emitted optical intensity I for the proposed scheme and conventional GLIM-OFDM schemes are considered to be equal, and $I = 1/2\sqrt{\pi}$. Consequently, the values of s_1 and s_2 are chosen to be $1/\sqrt{2\pi}$ and $1/2\pi^{3/2}$, respectively. The VLC channel matrices for two scenarios of 4×4 MIMO setups and one scenario of a 8×8 MIMO setup are given as [65, 71]

$$\mathbf{H}_1 = 10^{-5} \times \begin{pmatrix} 0.3489 & 0.3288 & 0.3104 & 0.3288 \\ 0.3288 & 0.3489 & 0.3288 & 0.3104 \\ 0.3104 & 0.3288 & 0.3489 & 0.3288 \\ 0.3288 & 0.3104 & 0.3288 & 0.3489 \end{pmatrix}, \tag{4.23}$$

$$\mathbf{H}_2 = 10^{-6} \times \begin{pmatrix} 0.5356 & 0.6831 & 0.3838 & 0.5762 \\ 0.3354 & 0.3440 & 0.5461 & 0.5121 \\ 0.3414 & 0.3161 & 0.5987 & 0.6031 \\ 0.6958 & 0.5614 & 0.4428 & 0.2052 \end{pmatrix}, \tag{4.24}$$

$$\mathbf{H}_3 = 10^{-6} \times \begin{pmatrix} 0.377 & 0.483 & 0.446 & 0.523 & 0.400 & 0.466 & 0.273 & 0.430 \\ 0.455 & 0.407 & 0.395 & 0.427 & 0.384 & 0.362 & 0.304 & 0.141 \\ 0.236 & 0.243 & 0.300 & 0.136 & 0.356 & 0.384 & 0.388 & 0.382 \\ 0.316 & 0.202 & 0.300 & 0.119 & 0.353 & 0.164 & 0.349 & 0.478 \\ 0.211 & 0.206 & 0.270 & 0.266 & 0.327 & 0.362 & 0.428 & 0.426 \\ 0.240 & 0.224 & 0.285 & 0.343 & 0.304 & 0.338 & 0.426 & 0.450 \\ 0.391 & 0.501 & 0.388 & 0.413 & 0.345 & 0.344 & 0.312 & 0.122 \\ 0.490 & 0.397 & 0.401 & 0.389 & 0.350 & 0.338 & 0.315 & 0.153 \end{pmatrix}. \quad (4.25)$$

Figure 18 on the following page and Figure 19 on the next page present the average BER performance of the proposed MW-OFDM with $P = 4$ and $L = 2$, compared to the conventional 4×4 GLIM-OFDM in [64, 65] for spectral efficiencies of 2, 3 and 4 bpcu. In Figure 18 on the following page, the BER results of the schemes are provided over $\mathbf{H}_1$ given in Eq. (4.23), while Figure 19 on the next page describes the BER curves over $\mathbf{H}_2$ given in Eq. (4.24).

It can be indicated from Figure 18 on the following page and Figure 19 on the next page that the proposed MW-OFDM can achieve much better BER performance compared to the conventional GLIM-OFDM. For instance, at the BER of 10^{-5} in Figure 18 on the following page, the required SNR values for the GLIM-OFDM scheme are 48.5, 53 and 55 dB in order to provide spectral efficiencies of 2, 3 and 4 bpcu, respectively. Whereas, by using the proposed MW-OFDM scheme, the required SNR values to obtain 2, 3 and 4 bpcu are decreased to 31, 39 and 43.5 dB, respectively. This indicates that the proposed scheme can improve the BER performance by 17.5 dB, 14 dB and 11.5 dB for spectral efficiencies of 2, 3 and 4 bpcu, respectively. In Figure 19 on the next page, the proposed scheme enhances the BER performance to provide these three reference bpcu values at the BER of 10^{-5} by 11 dB, 7 dB and 4.5 dB, respectively, in a comparison with the conventional GLIM-OFDM.

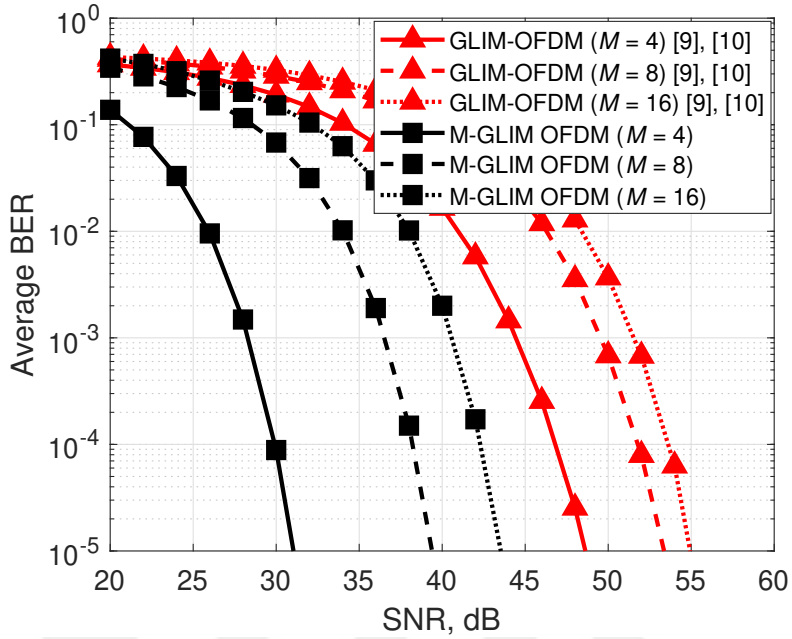

Figure 18: BER performance of the proposed MW-OFDM and conventional GLIM-OFDM for 2 (straight), 3 (dashed) and 4 (dotted) bpcu over channel $\mathbf{H}_1$.

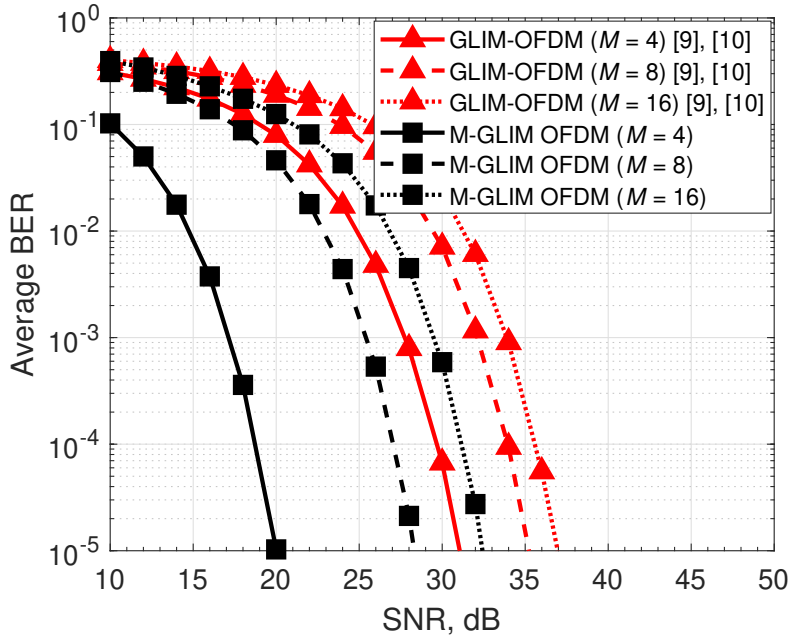

Figure 19: BER performance of the proposed MW-OFDM and conventional GLIM-OFDM for 2 (straight), 3 (dashed) and 4 (dotted) bpcu over channel $\mathbf{H}_2$.

Figure 20, we depict the BER performance of the proposed MW-OFDM scheme with $P = 8$ and $L = 4$, compared to the 8×8 GLIM-OFDM in [66] over $\mathbf{H}_3$ given in Eq. (4.25). The BER results in Figure 20 are obtained for the spectral efficiencies of 4, 6 and 8 bpcu, where two samples are simultaneously transmitted using 4-QAM, 8-QAM and 16-QAM, respectively. It can be shown from the results in this figure that the proposed MW-OFDM scheme achieves a better BER performance than the GLIM-OFDM for the same spectral efficiency. For instance, the proposed scheme improves the BER performance by 11, 7 and 6 dB for the spectral efficiencies of 4, 6 and 8 bpcu, respectively, compared to the GLIM-OFDM scheme.

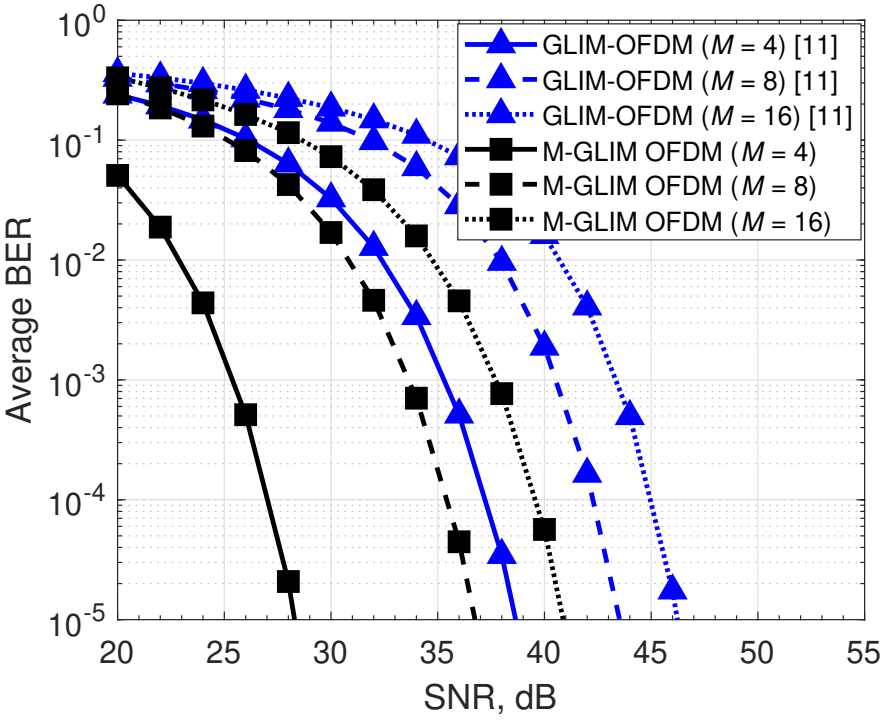

Figure 20: BER performance of the proposed MW-OFDM and conventional GLIM-OFDM for 4 (straight), 6 (dashed) and 8 (dotted) bpcu over channel $\mathbf{H}_3$.

It can be observed from these results that the proposed scheme significantly outperforms the conventional GLIM-OFDM schemes for different spectral efficiencies and over

different MIMO VLC channels scenarios. Furthermore, the proposed scheme offers a significant reduction in the decoding complexity at a required half number of LEDs compare to the existing GLIM-OFDM schemes as indicated in Section 4.4 on page 48.

CHAPTER V

CONCLUSIONS

In this thesis, we have focused on improving the spectral efficiency and BER performance for MIMO VLC systems in both the single-carrier and multi-carrier. Firstly, We proposed a novel FGSM scheme for single-carrier MIMO in order to improve the average SER performance and spectral efficiency of the VLC systems. Then, we have proposed two schemes for the multi-carrier MIMO VLC systems. We proposed an adaptive algorithm for the MIMO U-OFDM system to provide a significant spectral efficiency improvement over the VLC channels. Then, we proposed an MW-OFDM scheme to improve the BER performance of the MIMO VLC systems as well as achieve a significant reduction of the decoding complexity. The conclusions of this thesis can be summarized as follows:

In Chapter 2, a novel FGSM system has been proposed in order to achieve better average SER and higher spectral efficiency compared to ASM with a fixed total number of LEDs. For the proposed FGSM system, the closed-form expression of the approximate average SER has been derived and confirmed by Monte-Carlo simulation, as well as, its decoding complexity has been analyzed. At the expense of almost no extra cost in decoding complexity, the proposed system provides improvements up to 9.5 dB in SNR while achieving up to 46.2% increase in spectral efficiency [76].

In Chapter 3, we have proposed an adaptive transmission mechanism for the MIMO U-OFDM VLC system over different realistic VLC channel setups. The proposed adaptive transmission system has been designed to maximize the spectral efficiency of the system. The obtained spectral efficiency improvement is a result of switching between RC, SM and SMUX MIMO modes by satisfying the target BER based on the received SNR. Moreover, switching between different MIMO system setups has been considered for further spectral

efficiency improvement. Our simulation results have demonstrated that the proposed adaptive system provides a significant spectral efficiency improvement compared to stand-alone modes/setups [71].

In Chapter 4, a novel MW-OFDM scheme has been proposed to overcome the restriction on the number of LEDs and enhance the average BER performance in a comparison with existing GLIM-OFDM schemes. The proposed MW-OFDM transmits the magnitudes and wrap-phases of the complex OFDM samples, while a low complexity ML estimator has been derived. At the same spectral efficiency, the proposed MW-OFDM scheme can achieve a BER performance improvement up to 17.5 dB and reduce the decoding complexity up to 96%, while requires only a half number of LEDs in a comparison with the existing GLIM-OFDM schemes [77].

Bibliography

[1] L. E. M. Matheus, A. B. Vieira, L. F. M. Vieira, M. A. M. Vieira, and O. Gnawali, "Visible light communication: Concepts, applications and challenges," *IEEE Communications Surveys & Tutorials*, vol. 21, no. 4, pp. 3204–3237, Fourthquarter 2019.

[2] G. Held, *Introduction to Light Emitting Diode Technology and Applications*. Boca Raton, FL, USA: CRC Press, 2016.

[3] Z. Ghassemlooy, L. N. Alves, S. Zvanovec, and M.-A. Khalighi, *Visible Light Communications: Theory and Applications*. CRC Press, 2017.

[4] Z. Wang, Q. Wang, W. Huang, and Z. Xu, *Visible Light Communications: Modulation and Signal Processing*. Hoboken, NJ, USA: Wiley, 2017.

[5] R. Mesleh, H. Elgala, and H. Haas, "On the performance of different ofdm based optical wireless communication systems," *IEEE/OSA Journal of Optical Communications and Networking*, vol. 3, no. 8, pp. 620–628, Aug. 2011.

[6] M. Uysal, C. Capsoni, Z. Ghassemlooy, A. Boucouvalas, , and E. Udvary, *Optical Wireless Communications: An Emerging Technology*. Springer, 2016.

[7] T. Fath and H. Haas, "Performance comparison of mimo techniques for optical wireless communications in indoor environments," *IEEE Transactions on Communications*, vol. 61, no. 2, pp. 733–742, Feb. 2013.

[8] Y. Zhu, W. Liang, J. Zhang, and Y. Zhang, "Space-collaborative constellation designs for mimo indoor visible light communications," *IEEE Photonics Technology Letters*, vol. 27, no. 15, pp. 1667–1670, Aug. 2015.

[9] K. Ying, H. Qian, R. J. Baxley, and S. Yao, "Joint optimization of precoder and equalizer in mimo vlc systems," *IEEE Journal on Selected Areas in Communications*, vol. 33, no. 9, pp. 1949–1958, Sep. 2015.

[10] S. Al-Ahmadi, O. Maraqa, M. Uysal, and S. M. Sait, "Multi-user visible light communications: State-of-the-art and future directions," *IEEE Access*, vol. 6, pp. 70555–70571, 2018.

[11] S. Arnon, J. Barry, G. Karagiannidis, R. Schober, and M. Uysal, *Advanced Optical Wireless Communication Systems*. USA: Cambridge University Press, 1st ed., 2012.

[12] Z. Ghassemlooy, W. Popoola, and S. Rajbhandari, *Optical Wireless Communications: System and Channel Modelling with MATLAB*. USA: CRC Press, Inc., 1st ed., 2012.

[13] S. Arnon, *Visible Light Communication*. USA: Cambridge University Press, 1st ed., 2015.

[14] K. Asatani and T. Kimura, "Analyses of led nonlinear distortions," *IEEE Journal of Solid-State Circuits*, vol. 13, no. 1, pp. 125–133, Feb. 1978.

[15] H. Q. Nguyen, J. . Choi, M. Kang, Z. Ghassemlooy, D. H. Kim, S. . Lim, T. . Kang, and C. G. Lee, "A matlab-based simulation program for indoor visible light communication system," in *2010 7th International Symposium on Communication Systems, Networks Digital Signal Processing (CSNDSP 2010)*, pp. 537–541, July 2010.

[16] Shihe Long, M. Khalighi, M. Wolf, S. Bourennane, and Z. Ghassemlooy, "Channel characterization for indoor visible light communications," in *2014 3rd International Workshop in Optical Wireless Communications (IWOW)*, pp. 75–79, Sep. 2014.

[17] K. Lee, H. Park, and J. R. Barry, "Indoor channel characteristics for visible light communications," *IEEE Communications Letters*, vol. 15, no. 2, pp. 217–219, Feb. 2011.

[18] J. Ding, C. I, and Z. Xu, "Indoor optical wireless channel characteristics with distinct source radiation patterns," *IEEE Photonics Journal*, vol. 8, no. 1, pp. 1–15, Feb. 2016.

[19] H. Schulze, "Frequency-domain simulation of the indoor wireless optical communication channel," *IEEE Transactions on Communications*, vol. 64, no. 6, pp. 2551–2562, June 2016.

[20] C. Chen, D. Basnayaka, and H. Haas, "Non-line-of-sight channel impulse response characterisation in visible light communications," in *2016 IEEE International Conference on Communications (ICC)*, pp. 1–6, May 2016.

[21] A. Al-Kinani, C. Wang, H. Haas, and Y. Yang, "Characterization and modeling of visible light communication channels," in *2016 IEEE 83rd Vehicular Technology Conference (VTC Spring)*, pp. 1–5, May 2016.

[22] A. Al-Kinani, C. Wang, H. Haas, and Y. Yang, "A geometry-based multiple bounce model for visible light communication channels," in *2016 International Wireless Communications and Mobile Computing Conference (IWCMC)*, pp. 31–37, Sep. 2016.

[23] S. P. Rodriguez, R. P. Jimenez, B. R. Mendoza, F. J. L. Hernandez, and A. J. A. Alfonso, "Simulation of impulse response for indoor visible light communications using 3d cad models," *EURASIP Journal on Wireless Communications and Networking*, no. 7, pp. 1–10, Jan. 2013.

[24] J. Rufo, J. Rabadan, V. Guerra, and R. Perez-Jimenez, "Brdf models for the impulse response estimation in indoor optical wireless channels," *IEEE Photonics Technology Letters*, vol. 29, no. 17, pp. 1431–1434, Sep. 2017.

[25] M. Uysal, F. Miramirkhani, O. Narmanlioglu, T. Baykas, and E. Panayirci, "Ieee 802.15.7r1 reference channel models for visible light communications," *IEEE Communications Magazine*, vol. 55, no. 1, pp. 212–217, Jan. 2017.

[26] F. Miramirkhani and M. Uysal, "Channel modeling and characterization for visible light communications," *IEEE Photonics Journal*, vol. 7, no. 6, pp. 1–16, Dec. 2015.

[27] F. Miramirkhani, M. Uysal, and E. Panayirci, "Novel channel models for visible light communications," in *Broadband Access Communication Technologies IX*, vol. 9387, pp. 150–162, SPIE, Feb. 2015.

[28] O. Narmanlioglu, R. C. Kizilirmak, T. Baykas, and M. Uysal, "Link adaptation for mimo ofdm visible light communication systems," *IEEE Access*, vol. 5, pp. 26006–26014, 2017.

[29] T. Komine and M. Nakagawa, "Fundamental analysis for visible-light communication system using led lights," *IEEE Transactions on Consumer Electronics*, vol. 50, no. 1, pp. 100–107, June 2004.

[30] S. Dimitrov and H. Haas, *Principles of LED Light Communications: Towards Networked Li-Fi*. Cambridge University Press, 2015.

[31] G. Stepniak, M. Schüppert, and C. Bunge, "Advanced modulation formats in phosphorous led vlc links and the impact of blue filtering," *Journal of Lightwave Technology*, vol. 33, no. 21, pp. 4413–4423, Nov. 2015.

[32] D. J. F. Barros, S. K. Wilson, and J. M. Kahn, "Comparison of orthogonal frequency-division multiplexing and pulse-amplitude modulation in indoor optical wireless links," *IEEE Transactions on Communications*, vol. 60, no. 1, pp. 153–163, Jan. 2012.

[33] "Ieee standard for local and metropolitan area networks–part 15.7: Short-range wireless optical communication using visible light," *IEEE Std 802.15.7-2011*, pp. 1–309, Sep. 2011.

[34] A. Nuwanpriya, S. Ho, J. A. Zhang, A. J. Grant, and L. Luo, "Pam-scfde for optical wireless communications," *Journal of Lightwave Technology*, vol. 33, no. 14, pp. 2938–2949, July 2015.

[35] Y. Tanaka, T. Komine, S. Haruyama, and M. Nakagawa, "Indoor visible communication utilizing plural white leds as lighting," in *12th IEEE International Symposium on Personal, Indoor and Mobile Radio Communications (PIMRC)*, vol. 2, (San Diego, CA), pp. 81–85, 2001.

[36] H. Elgala, R. Mesleh, and H. Haas, "Indoor broadcasting via white leds and ofdm," *IEEE Transactions on Consumer Electronics*, vol. 55, no. 3, pp. 1127–1134, Aug. 2009.

[37] S. B. Weinstein, "The history of orthogonal frequency-division multiplexing [history of communications]," *IEEE Communications Magazine*, vol. 47, no. 11, pp. 26–35, Nov. 2009.

[38] J. Armstrong and A. J. Lowery, "Power efficient optical ofdm," *Electronics Letters*, vol. 42, no. 6, pp. 370–372, Mar. 2006.

[39] J. Armstrong, "Ofdm for optical communications," *Journal of Lightwave Technology*, vol. 27, no. 3, pp. 189–204, Feb. 2009.

[40] R. C. Kizilirmak, O. Narmanlioglu, and M. Uysal, "Relay-assisted ofdm-based visible light communications," *IEEE Transactions on Communications*, vol. 63, no. 10, pp. 3765–3778, Oct. 2015.

[41] D. Tsonev, S. Sinanovic, and H. Haas, "Novel unipolar orthogonal frequency division multiplexing (u-ofdm) for optical wireless," in *2012 IEEE 75th Vehicular Technology Conference (VTC Spring)*, pp. 1–5, 2012.

[42] S. Rajagopal, R. D. Roberts, and S. Lim, "Ieee 802.15.7 visible light communication: modulation schemes and dimming support," *IEEE Communications Magazine*, vol. 50, no. 3, pp. 72–82, Mar. 2012.

[43] N. Fernando, Y. Hong, and E. Viterbo, "Flip-ofdm for unipolar communication systems," *IEEE Transactions on Communications*, vol. 60, no. 12, pp. 3726–3733, Dec. 2012.

[44] D. Tsonev, S. Videv, and H. Haas, "Unlocking spectral efficiency in intensity modulation and direct detection systems," *IEEE Journal on Selected Areas in Communications*, vol. 33, no. 9, pp. 1758–1770, Sep. 2015.

[45] S. P. Alaka, T. L. Narasimhan, and A. Chockalingam, "Generalized spatial modulation in indoor wireless visible light communication," in *2015 IEEE Global Communications Conference (GLOBECOM)*, pp. 1–7, 2015.

[46] J. Wang, J. Zhu, S. Lin, and J. Wang, "Adaptive spatial modulation based visible light communications: Ser analysis and optimization," *IEEE Photonics Journal*, vol. 10, no. 3, pp. 1–14, June 2018.

[47] C. He, T. Q. Wang, and J. Armstrong, "Performance of optical receivers using photodetectors with different fields of view in a mimo aco-ofdm system," *Journal of Lightwave Technology*, vol. 33, no. 23, pp. 4957–4967, Dec. 2015.

[48] Q. Wang, Z. Wang, and L. Dai, "Multiuser mimo-ofdm for visible light communications," *IEEE Photonics Journal*, vol. 7, no. 6, pp. 1–11, Dec. 2015.

[49] M. O. Damen, O. Narmanlioglu, and M. Uysal, "Comparative performance evaluation of mimo visible light communication systems," in *2016 24th Signal Processing and Communication Application Conference (SIU)*, pp. 525–528, 2016.

[50] J. Vucic, C. Kottke, S. Nerreter, K. Langer, and J. W. Walewski, "513 mbit/s visible light communications link based on dmt-modulation of a white led," *Journal of Lightwave Technology*, vol. 28, no. 24, pp. 3512–3518, Dec. 2010.

[51] P. W. Berenguer, V. Jungnickel, and J. K. Fischer, "The benefit of frequency-selective rate adaptation for optical wireless communications," in *2016 10th International Symposium on Communication Systems, Networks and Digital Signal Processing (CSNDSP)*, pp. 1–6, 2016.

[52] L. Wu, Z. Zhang, J. Dang, and H. Liu, "Adaptive modulation schemes for visible light communications," *Journal of Lightwave Technology*, vol. 33, no. 1, pp. 117–125, Jan. 2015.

[53] M. Wang, J. Wu, W. Yu, H. Wang, J. Li, J. Shi, and C. Luo, "Efficient coding modulation and seamless rate adaptation for visible light communications," *IEEE Wireless Communications*, vol. 22, no. 2, pp. 86–93, Apr. 2015.

[54] J. He, J. He, and J. Shi, "An enhanced adaptive scheme with pairwise coding for ofdm-vlc system," *IEEE Photonics Technology Letters*, vol. 30, no. 13, pp. 1254–1257, July 2018.

[55] K. Park, Y. Ko, and M. Alouini, "On the power and offset allocation for rate adaptation of spatial multiplexing in optical wireless mimo channels," *IEEE Transactions on Communications*, vol. 61, no. 4, pp. 1535–1543, Apr. 2013.

[56] P. F. Mmbaga, J. Thompson, and H. Haas, "Performance analysis of indoor diffuse vlc mimo channels using angular diversity detectors," *Journal of Lightwave Technology*, vol. 34, no. 4, pp. 1254–1266, Feb. 2016.

[57] I. Tavakkolnia, C. Chen, R. Bian, and H. Haas, "Energy-efficient adaptive mimo-vlc technique for indoor lifi applications," in *2018 25th International Conference on Telecommunications (ICT)*, pp. 331–335, 2018.

[58] Y. Hong, T. Wu, and L. Chen, "On the performance of adaptive mimo-ofdm indoor visible light communications," *IEEE Photonics Technology Letters*, vol. 28, no. 8, pp. 907–910, Apr. 2016.

[59] H. Elgala and T. D. C. Little, "P-ofdm: Spectrally efficient unipolar ofdm," in *IEEE Optical Fiber Communication (OFC 2014) Conference*, pp. 1–3, 2014.

[60] H. Elgala and T. D. C. Little, "Polar-based ofdm and sc-fde links toward energy-efficient gbps transmission under im-dd optical system constraints [invited]," *IEEE/OSA Journal of Optical Communications and Networking*, vol. 7, no. 2, pp. A277–A284, Feb. 2015.

[61] S. Guo, K. Park, and M. Alouini, "Adaptive power allocation for distortion minimization in generalized polar optical wireless communications," *IEEE Transactions on Communications*, vol. 67, no. 12, pp. 8545–8556, Dec. 2019.

[62] T. L. Narasimhan, R. Tejaswi, and A. Chockalingam, "Quad-led and dual-led complex modulation for visible light communication," *arXiv*, 2015.

[63] A. K. Gupta and A. Chockalingam, "Performance of mimo modulation schemes with imaging receivers in visible light communication," *Journal of Lightwave Technology*, vol. 36, no. 10, pp. 1912–1927, May 2018.

[64] E. Basar, E. Panayirci, M. Uysal, and H. Haas, "Generalized led index modulation optical ofdm for mimo visible light communications systems," in *2016 IEEE International Conference on Communications (ICC)*, pp. 1–5, 2016.

[65] A. Yesilkaya, E. Basar, F. Miramirkhani, E. Panayirci, M. Uysal, and H. Haas, "Optical mimo-ofdm with generalized led index modulation," *IEEE Transactions on Communications*, vol. 65, no. 8, pp. 3429–3441, Aug. 2017.

[66] M. Le Tran, S. Kim, T. Ketseoglou, and E. Ayanoglu, "Led selection and map detection for generalized led index modulation," *IEEE Photonics Technology Letters*, vol. 30, no. 19, pp. 1695–1698, Oct. 2018.

[67] J. G. Proakis and M. Salehi, *Digital Communications*. New York, USA: McGrawHill, Inc, 5th ed., 2008.

[68] Z. B. Zabinsky, *Stochastic Adaptive Search for Global Optimization*. Kluwer Academic Publishers, 2003.

[69] G. H. Givens and J. A.-. Hoeting, *Computational statistics*. Wiley, 2013.

[70] L. Bai and J. Choi, *Low Complexity MIMO Detection*. Boston, MA, USA: Springer Publishing Company, 2012.

[71] M. Al-Nahhal, E. Basar, and M. Uysal, "Adaptive unipolar mimo-ofdm for visible light communications," in *2019 European Conference on Networks and Communications (EuCNC)*, pp. 73–77, 2019.

[72] Y. S. Cho, J. Kim, W. Y. Yang, and C. G. Kang, *MIMO-OFDM Wireless Communications with MATLAB*. Wiley Publishing, 2010.

[73] E. Basar, M. Wen, R. Mesleh, M. Di Renzo, Y. Xiao, and H. Haas, "Index modulation techniques for next-generation wireless networks," *IEEE Access*, vol. 5, pp. 16693–16746, 2017.

[74] M. T. Alresheedi, A. T. Hussein, and J. M. H. Elmirghani, "Uplink design in vlc systems with ir sources and beam steering," *IET Communications*, vol. 11, no. 3, pp. 311–317, Feb. 2017.

[75] I. Al-Nahhal, O. A. Dobre, E. Basar, C. Moloney, and S. Ikki, "A fast, accurate, and separable method for fitting a gaussian function [tips tricks]," *IEEE Signal Processing Magazine*, vol. 36, no. 6, pp. 157–163, Nov. 2019.

[76] M. Al-Nahhal, E. Basar, and M. Uysal, "Flexible generalized spatial modulation for visible light communications," *Submitted to IEEE Transactions on Vehicular Technology*, 2020.

[77] M. Al-Nahhal, E. Basar, and M. Uysal, "Magnitude and wrap-phase ofdm for mimo visible light communication systems," *To be submitted to IEEE Communication Letters*, 2020.

VITA

Mohamed Al-Nahhal was born in Sharkia, Egypt. He received the B.Sc. degree (Honors) in 2013 from the Electronics and Electrical Communications Engineering Department, Faculty of Engineering, Al-Azhar University, Cairo, Egypt. He received the excellence award in the last four years of his undergraduate study. He joined as a research assistant at Communication Theory and Technologies (CT&T) Research Group under the supervision of Prof. Murat Uysal at Özyeğin University, Istanbul, Turkey, since 2017. Currently, he is a teaching assistant at Department of Electrical and Electronics Engineering at Özyeğin University, Istanbul, Turkey. He worked as a radar and surveillance technical engineer at Aiactive Technologies Company, Red Sea, Egypt in 2015. Since 2016, he worked as a teaching assistant at Al Alson Institute, Cairo, Egypt; teaching assistant at Bilbis Higher Institute for Engineering (BHIE), Sharkia, Egypt; researcher in a project which is funded by National Telecommunications Regulatory Authority (NTRA), Giza, Egypt (the biggest organization in telecommunication field in Egypt). His research interests include wireless communications, performance analysis, visible light communications, millimeter wave communications, MIMO, OFDM, spatial modulation, free space optical communications. He served as a reviewer for the Institute of Electrical & Electronics Engineers (IEEE) journals and conferences as well as Optical Society of America (OSA) and Elsevier journals. He is a student member of IEEE communications society.